

## Review

# Advances in Soft Bioelectronics for Brain Research and Clinical Neuroengineering

Sung-Hyuk Sunwoo,<sup>1,2,6</sup> Sang Ihn Han,<sup>1,2,6</sup> Hyunwoo Joo,<sup>1,2,6</sup> Gi Doo Cha,<sup>1,2</sup> Dokyoon Kim,<sup>1,3</sup> Seung Hong Choi,<sup>1,4</sup> Taeghwan Hyeon,<sup>1,2,\*</sup> and Dae-Hyeong Kim<sup>1,2,5,\*</sup>

## SUMMARY

Recent advances in bioelectronics, such as skin-mounted electroencephalography sensors, multi-channel neural probes, and closed-loop deep brain stimulators, have enabled electrophysiological brain activities to be both monitored and modulated. Despite this remarkable progress, major challenges remain, which stem from the inherent mechanical, chemical, and electrical differences that exist between brain tissues and bioelectronics. New approaches are therefore required to address these mismatches between biotic and abiotic systems. Here, we review recent technological advances that minimize such mismatches by using unconventional soft materials, such as silicon/metal nanowires, functionalized hydrogels, and stretchable conductive nanocomposites, as well as customized fabrication processes and novel device designs. The resulting novel, soft bioelectronic devices provide new opportunities for brain research and clinical neuroengineering.

## INTRODUCTION

Brain diseases and disorders, including neurodegenerative, psychiatric, oncological, and neurodevelopmental, as well as injuries that require neurorehabilitation, have highlighted a clinical role and need for neurotechnologies that can monitor and modulate brain activity. Such technologies might also have wider clinical applications, given that electrical signals from the brain coordinate peripheral nerves and electrically active organs, including the heart,<sup>1</sup> muscles,<sup>2</sup> gastrointestinal organs,<sup>3</sup> and endocrine organs.<sup>4</sup> However, a key challenge for neurotechnologies is to provide faithful, minimally invasive, and long-term recordings of electrical signals from the nervous system in often-changing physiological conditions, for example during different developmental, behavioral, and neurological states, and in pathological or trauma conditions.

Bioelectronic technologies to date have facilitated our understanding of abnormal electrophysiological signals as well as the recognition of subtle pathological symptoms, the modulation of epileptic neuronal activities, and the treatment of various intractable neurological diseases. They include recording devices for skin-based electroencephalography (EEG),<sup>5</sup> epicortical electrocorticography (ECoG),<sup>6,7</sup> and intracortical encephalography (ICE).<sup>8,9</sup> Optogenetic<sup>10</sup> and thermal<sup>11</sup> stimulation devices have also been devised as new paradigms for neural modulation. The integration of wireless device components and the miniaturization of an entire implantable system have also significantly accelerated such advances.<sup>12</sup>

Despite these advances, maintaining the long-term biocompatibility, reliability, and stability of such bioelectronic devices *in vivo* remains a key challenge. These issues are largely due to the different mechanical characteristics, called “mechanical

## Progress and Potential

Advances in bioelectronics for neuroscience and neuroengineering have enabled continuous monitoring of electrophysiological signals and feedback modulation of abnormal brain activities. Despite such progress, there remain issues in terms of long-term high-quality neural interfacing, mainly owing to inherent mechanical, chemical, and electrical mismatches between the device and the brain tissue. New approaches, therefore, are required to address these discrepancies between the biotic and abiotic system. This review introduces technological advances that potentially solve such issues by using soft materials and devices. Specifically, we summarize recent progress in soft materials, such as nanoscale materials, conductive polymers, functionalized hydrogels, and stretchable conductive nanocomposites. These unconventional materials, combined with customized processing techniques and device designs, provide novel soft device solutions for brain science and clinical neuroengineering.



mismatches," that exist between biological tissue and the materials used in bioelectronic devices. In addition, there are notable mismatches between the chemical<sup>13</sup> and electrical<sup>14,15</sup> properties of these devices and brain tissue; while brain tissue consists of organic structures that have a high water content in which ions control signal transmission, bioelectronic devices are typically composed of dry inorganic materials in which electrons serve as information transmitters.

In recent years, the limitations of conventional bioelectronics have been addressed by engineering better materials and by designing advanced devices, heralding the advent of soft bioelectronics. In this review, we discuss how the development of new soft bioelectronics aims to mitigate these limitations, focusing on material designs, fabrication, and device choice for diverse applications. We also describe how soft bioelectronics creates new opportunities for the long-term, high-quality monitoring of brain signals and for the use of controlled feedback therapies to treat brain diseases. Additionally, we highlight device applications that have shown promise in clinical studies, discuss issues associated with the clinical translation of soft bioelectronics, and end with future directions for the improved design of soft bioelectronics.

## CHALLENGES FACED BY CONVENTIONAL BIOELECTRONICS

A key issue in conventional bioelectronics is a mechanical mismatch,<sup>16,17</sup> which mainly derives from two important contributors of a device, namely its material properties and its geometry, which are interdependent. Young's modulus, which defines how a material will strain (that is, deform) under stress (as measured by force/unit area), differs by several orders of magnitude between conventional rigid bioelectronic devices (which have moduli in the order of GPa) and soft brain tissues (which have moduli in the order of kPa).<sup>18</sup> The overall size and design of electrodes also affect the bending stiffness, which is proportional to Young's modulus, the width of the probe, and the third power of thickness of the probe.<sup>19</sup> As a result, rigid implanted devices, conventionally made of tungsten wires or silicon probes, can cause chronic stressors, which over a long period of time can cause significant damage to brain tissue as well as to the implant itself, generating functional failures in both (Figure 1A). In contrast, soft bioelectronics can better endure the same stressors (Figure 1B).

Device implantation, such as for intracortical recording, can also cause damage to an implant and the surrounding tissue during the process of implantation (for example through scarring, bleeding, and inflammatory reactions). There are also long-term effects, such as the isolation of a bioelectronic device due to fibrous scar formation and subsequent chronic inflammation, which can include protein attachment, astrocyte recruitment, and fibrosis around implanted electrodes. The formation of these fibrous tissues increases the electrical impedance at the tissue-electrode interface and the degradation of measured electrical signals (Figure 1C). The geometry and size of an implant also determine the extent of damage. For example, larger bioelectrodes exhibit higher mechanical mismatch and cause greater mechanical damage.<sup>20</sup> The vigorous micromotions of the brain also cause chronic stress on the tissue.<sup>21,22</sup> Moreover, the mechanical stress on the implanted electrode can lead to a failure of the encapsulation layer, causing electrical current to leak to non-targeted brain regions<sup>23</sup> and making the electrodes vulnerable to corrosion.

In the case of less invasive, skin-mounted EEG measurement devices, the main challenge is to maintain high-quality, long-term conformal contact between the bioelectronics and the elastic, wrinkled skin.<sup>24,25</sup> Due to the stiffness of the constituent

---

<sup>1</sup>Center for Nanoparticle Research, Institute for Basic Science (IBS), Seoul 08826, Republic of Korea

<sup>2</sup>School of Chemical and Biological Engineering, Institute of Chemical Processes, Seoul National University, Seoul 08826, Republic of Korea

<sup>3</sup>Department of Bionano Engineering and Bionanotechnology, Hanyang University, Ansan 15588, Republic of Korea

<sup>4</sup>Department of Radiology, Seoul National University College of Medicine, Seoul 03080, Republic of Korea

<sup>5</sup>Department of Materials Science and Engineering, Seoul National University, Seoul 08826, Republic of Korea

<sup>6</sup>These authors contributed equally

\*Correspondence: [thyeon@snu.ac.kr](mailto:thyeon@snu.ac.kr) (T.H.), [dkim98@snu.ac.kr](mailto:dkim98@snu.ac.kr) (D.-H.K.)

<https://doi.org/10.1016/j.matt.2020.10.020>

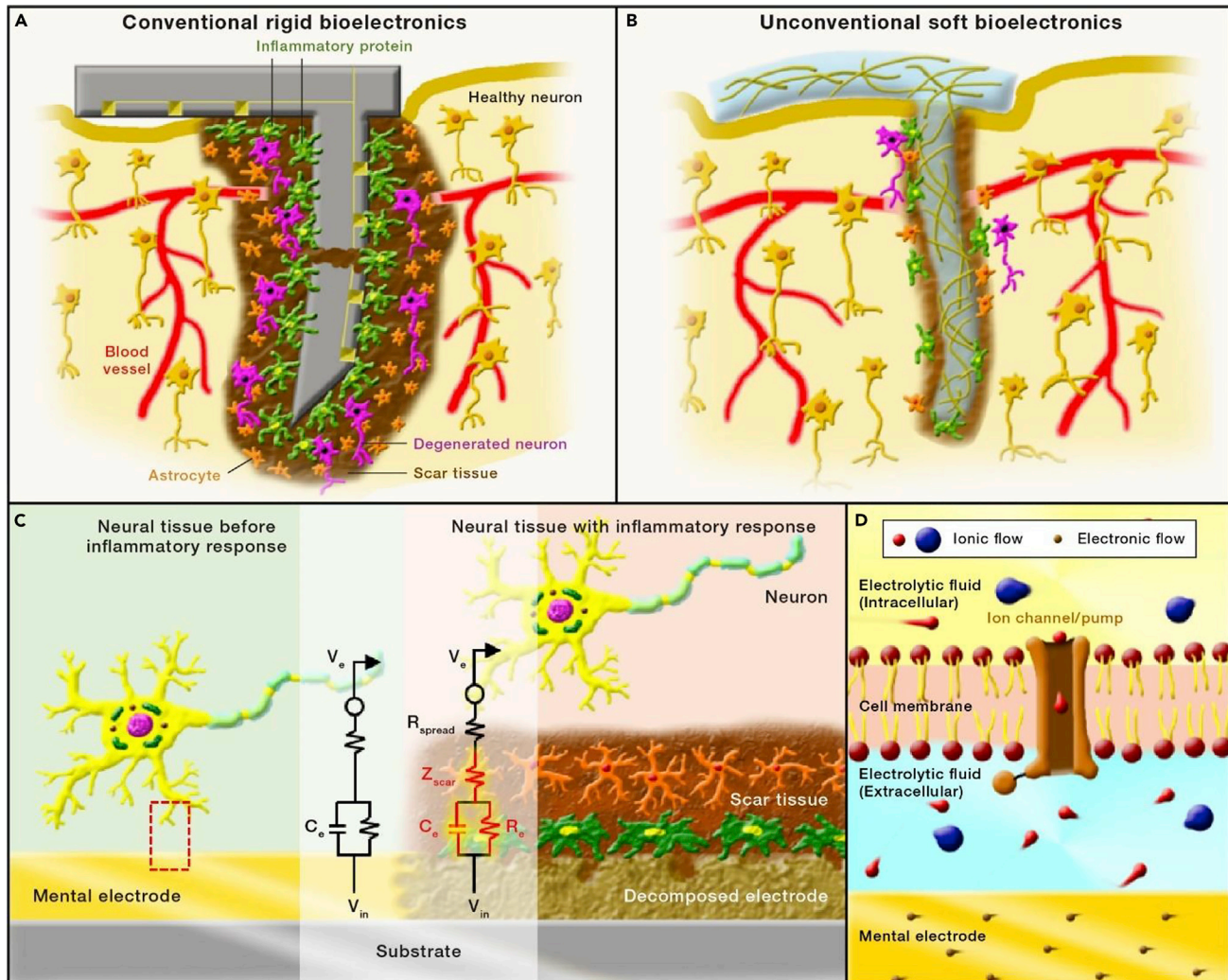


**Figure 1. Mechanical, Chemical, and Electrical Mismatches between Brain Tissue and Conventional Bioelectronics**

(A) Inflammatory reactions are caused by a conventional, rigid intracortical electrode (shaded gray). Inflammatory proteins (green) and astrocytes (orange) are recruited to the implantation site, and extensive scar tissue (brown) forms around the electrode. As a result, electrophysiological signals are isolated from the electrode because degenerated neurons (purple) block the signals transmitted from the active neurons (yellow) to the electrode.

(B) A soft intracortical bioelectrode produces a significantly reduced inflammatory reaction in comparison with that caused by a conventional intracortical bioelectrode because of reduced mismatches.

(C) Mechanism of device failure due to scar tissue formation. The overall impedance at the neural interface increases due to the effect of insulative scar tissue ( $Z_{scar}$ ), charge transfer resistance ( $R_e$ ), and capacitance ( $C_e$ ) change. The subcellular scale structure of the neural interfaces (red dotted box) is illustrated in (D).

(D) Differences in the electrical characteristics of a conventional metal electrode and biological tissue. In the extracellular fluid, an electrical signal is transmitted as an ionic current and in the electrode, as electron flow.

materials, conventional electrodes cannot perfectly follow the microscopic curvature of the wrinkled skin. Additionally, repetitive stretching of elastic skin often causes electrodes to delaminate from it. Such non-conformal contact with the skin surface can abruptly increase impedance and dramatically decrease the signal-to-noise ratio (SNR). Furthermore, the long-term attachment of rigid electrodes to the skin leads to skin irritation, necessitating the use of softer materials.<sup>26,27</sup>

Another key issue is a chemical mismatch caused by differences between the chemical composition of brain tissue and the inorganic materials used in conventional

bioelectronics. While brain tissue contains a large amount of water and is ion-rich, the inorganic materials used in bioelectronic devices can be hydrophobic in nature and can have low fluid permeability, causing low cellular affinity, which impedes cell attachment and cell-electrode interactions.<sup>28</sup>

The interface between a device's electrodes and brain tissue is called the neural interface, a solid electrode interface with an electrolytic solution where charge transfers occur between the ions in the fluid and the electrons in the electrode (Figure 1D). As with all such electrode/electrolyte systems, discontinuities in the implant/tissue interface distort the measured electrical signals. The degree of this distortion depends on differences in the junction potential of two interfacing partners (i.e., the extracellular fluid and electrode materials). Such discontinuity at the interface apparently increases the interfacial impedance, which decreases the SNR.<sup>29</sup> In addition to a poor SNR and distorted electrical recordings, current leakage from a damaged rigid electrode (Figure 1A) can result in undesirable electrochemical reactions, such as the electrolysis of water, the oxidation of materials, and the reduction of ions, which can also damage brain tissue.<sup>30</sup>

As we discuss in the remainder of this review, novel technological approaches are being developed that aim to minimize the aforementioned mechanical, chemical, and electrical differences between the conventional bioelectronic devices and brain tissue. These approaches are developing soft bioelectronic devices—based on unconventional materials, new fabrication processes, and device designs—that aim to be biocompatible, reliable, and stable over long time periods *in vivo*.

## UNCONVENTIONAL MATERIALS FOR SOFT BIOELECTRONICS

In this section, we discuss efforts to develop bioelectronics that minimize the mechanical, chemical, and electrical differences between tissues and devices through the use of unconventional soft materials (Figure 2A), the characteristics of which are summarized in Table 1.

### Reducing Stiffness with Ultrathin Materials

The mechanical stiffness of a material is highly dependent on its geometry; a conventional material processed into an ultrathin form (of  $<10\ \mu\text{m}$ )<sup>60,61</sup> will show a dramatic decrease in its stiffness. Importantly, reducing a material's thickness decreases its flexural rigidity without losing the original electrical properties of its bulk state.<sup>62,63,35</sup> Ultrathin materials thus become soft, exhibiting much smaller mechanical differences from brain tissue in terms of bending stiffness,<sup>64</sup> while still serving as an electronic device component with the properties of a conventional bulk-state material. As such, devices based on ultrathin materials can make soft, conformal contact with brain tissue, solving the problem of mechanical mismatch. Biocompatible metals, such as gold,<sup>64</sup> platinum,<sup>65</sup> iridium,<sup>66</sup> and their alloys, placed on flexible polymer substrates such as polyimide, parylene, and epoxy, have been used to generate flexible, ultrathin bioelectronics.

The geometry of ultrathin devices can be designed as a mesh structure to maximize the effect of ultrathin materials on the deformability of the device.<sup>10,67</sup> An ultrathin film with a large area has flexibility in one direction, whereas an ultrathin, line-shape film has flexibility in multiple directions, which is beneficial for ensuring the deformability of the device. For example, Liu et al. developed syringe-injectable electronics with a large area and a mesh-like design, and of sub-micrometer thickness (Figure 2B).<sup>31</sup> Although the mesh of this device is deformed and entangled inside the

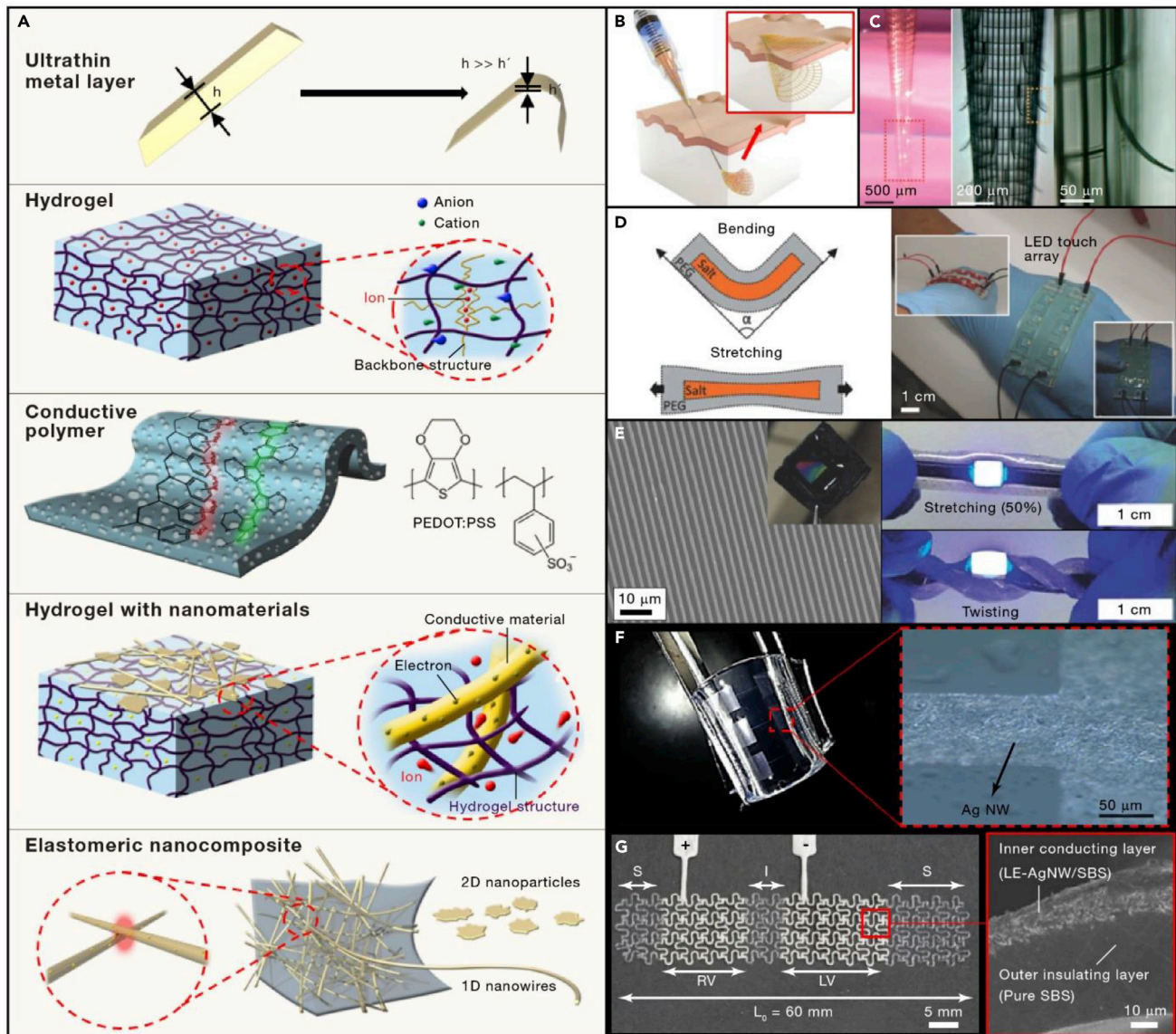


**Figure 2. Unconventional Materials for Soft Bioelectronics**

(A) Schematics of the unconventional soft materials used in soft bioelectronics.  
 (B) Illustration of the ultrathin mesh-shape macroporous electrode array. Reproduced with permission.<sup>31</sup> Copyright 2015, Springer Nature.  
 (C) Optical image of the syringe-injectable porous electronics. Reproduced with permission.<sup>19</sup> Copyright 2015, Springer Nature.  
 (D) Schematic illustration of the deformable PEG hydrogel matrix that contains ionic salts (left) and its application as a soft bioelectronic device (right). Reproduced with permission.<sup>32</sup> Copyright 2018, Wiley-VCH.  
 (E) Microscopic image of patterned PEDOT:PSS-based elastomer composite (left), optical image of patterned PEDOT:PSS (inset), and applied to an electrode (right). Reproduced with permission.<sup>33</sup> Copyright 2016, Wiley-VCH.  
 (F) An AgNW film that was transferred onto a hydrogel is mounted on a curved surface (left) and its magnified image shows the patterned AgNW network (right). Reproduced with permission.<sup>34</sup> Copyright 2014, American Chemical Society.  
 (G) Soft bioelectronics fabricated with the stretchable conductive nanocomposite composed of AgNWs and an elastomeric polymer. Reproduced with permission.<sup>35</sup> Copyright 2016, AAAS.

syringe before its injection, the original mesh design recovers after injection once it has relaxed inside the body's cavity. The multiple channels incorporated into this device's electronics enabled brain activity to be recorded across 16 channels in the hippocampus of anesthetized mice. Due to the soft mechanical nature of the device, which is compatible with brain tissue, minimal chronic immunoreactivity was

**Table 1. General Characteristics of Representative Unconventional Materials**

		Mechanical Property		Chemical Property		Electrical Property		Fabrication Resolution	References
		Softness <sup>a</sup>	Thickness	Biocompatibility	Lifetime	Impedance	Conductivity		
						( $\Omega$ , @1 KHz)	(S/cm)		
Metal layer	Au	rigid	very thin	compatible	long	high	very high	high	10,31,19
		~79 GPa				~1 M $\Omega$	411,000		
	Pt	rigid	very thin	compatible	long	low	high	high	36
		~168 GPa				~400 $\Omega$	94,300		
	IrOx	rigid	very thin	compatible	long	low	very high	high	36,37
		~530 GPa				~350 $\Omega$	213,000		
Conductive polymer	PEDOT:PSS	moderate	thin	moderate	moderate	low	moderate	moderate	36,38,39,40
		~2 GPa				~300 $\Omega$	10–1,000		
	PPy	moderate	thin	moderate	moderate	low	moderate	moderate	41,42,43,44
		~600 MPa				~100 $\Omega$	2–100		
Hydrogel	pure	very soft	moderate	compatible	short	high	very low	low	45,46,47
		~100 kPa				10 M $\Omega$	0.0001		
	conducting polymer fillers <sup>b</sup>	very soft	moderate	compatible	short	moderate	moderate	low	48,49,50
		~32 kPa				~15 k $\Omega$	~47.4		
	nanomaterial fillers <sup>b</sup>	very soft	moderate	compatible	short	moderate	low	low	34,51,52,49,53,54,55
		~100 kPa				~1.5 k $\Omega$	~0.1		
Elastomeric nanocomposite <sup>b</sup>		soft	moderate	moderate	moderate	moderate	high	low	56,57,58,35,59
		~4 MPa				~1 k $\Omega$	~72,000		
Conventional material	metal/silicon	rigid	thick	compatible	moderate	high	very high	high	
		~185 GPa				~1 M $\Omega$	411,000		

The detailed value and properties may vary depending on the material type and thickness.

<sup>a</sup>The value of bending stiffness may vary by thickness.

<sup>b</sup>The value may vary by filler materials.

observed over 5 weeks. This result shows a higher biocompatibility than conventional silicon probes. It has been known that silicon penetrating probes involve gliosis and lose their recording function rapidly (e.g., within 3 weeks<sup>68</sup>).

This two-dimensional (2D) mesh design can be extended into a three-dimensional (3D) design, such as a macroporous 3D network of nanoelectronics composed of silicon nanowires and ultrathin metal electrodes.<sup>19</sup> The high porosity and small feature size of the porous 3D mesh electronics (Figure 2C) enable them to be highly flexible and to conform closely with the target neural tissue, helping to minimize mechanically induced scarring and the recruitment of glial cells. The effective bending stiffness of this 3D mesh design is  $<0.64 \times 10^{-15} \text{ Nm}^2$ , which is four to seven orders of magnitude lower than that of conventional neural probes, based on Si,<sup>69</sup> carbon fiber,<sup>70</sup> and planar polyimide films.<sup>10,71</sup> Moreover, histological analyses after *in vivo* implantation of the porous 3D mesh electronics in rat somatosensory cortex showed normal neuronal densities in close proximity ( $<50 \mu\text{m}$ ) to the device, in contrast to typical neural probes.<sup>72,73</sup>

### Surface Coatings and Encapsulation

Although ultrathin electronic materials and porous mesh device structures can minimize mechanical mismatches between biotic and abiotic systems, the chemical

mismatches between these devices and brain tissue remain an issue, limiting their ability to provide long-term, stable recordings.<sup>45,74</sup> Here, we consider various surface coating and encapsulation strategies to bridge these chemical differences.

One strategy is to coat electrodes with a conducting polymer to provide a better interface between the tissue and the recording site. For example, when a film of poly(3,4-ethylenedioxythiophene) (PEDOT) is deposited on an electrode, its recording performance can be improved in terms of the SNR because the PEDOT film provides a low-impedance interface between the electrode and the tissue.<sup>45</sup>

Another strategy is to coat electrodes with bioactive materials. A bioactive coating can promote neuronal growth and cell adhesion. For example, nerve growth factor (NGF) can be doped with the conducting polymer to elicit specific biological interactions between the electrode materials and neurons.<sup>75</sup> Incorporation of NGF, which promotes the survival and differentiation of sensory and sympathetic neurons during development, in the electrode coating can promote better integration between the electrode and the neurons. When PC12 (rat pheochromocytoma) cells are cultured with the NGF-modified electrode, the cells adhere to the electrode and extended neurites, indicating the NGF-modified electrode is biologically active. Although these coating techniques can improve chronic recording performance, including higher SNR, by lowering electrode impedance, the mismatch between the electronics and ion-rich and water-rich brain tissues still exists and needs to be further improved.

Recently hydrogels, a network of polymer chains infiltrated with water, have gained attention due to their unique tissue-like mechanical properties, biocompatibility, and, more importantly, because of their high water content.<sup>46,76</sup> Hydrogels exhibit very low Young's modulus ( $\sim$ kPa)<sup>46</sup> compared with silicon, gold, platinum ( $\sim$ GPa),<sup>77,78,45</sup> or elastomers ( $\sim$ MPa).<sup>79</sup> The high water and ion content of a hydrogel can make a bioelectronic device compatible with the wet and ion-rich physiological environment *in vivo*, minimizing the chemical compositional mismatch between the electronics and the tissue.<sup>80</sup> The hydrophilicity of a hydrogel matrix also prevents the adsorption of proinflammatory proteins onto the electrode surface by inhibiting their hydrophobic domains from adhering to the surface, while hydrophilic protein attachment is deterred through the formation of a water layer on the device.<sup>81</sup>

Hydrogels have been incorporated into an electronic device via surface coating or encapsulation.<sup>82,83</sup> For example, the application of a hydrogel onto an EEG electrode produced a hydrating effect on the human scalp that could last for more than 8 h; it also increased the effective contact area due to the conformal contact of the soft hydrogel on the rough skin surface.<sup>82</sup> As a result, an electrode applied with hydrogel exhibits an impedance of  $15 \text{ k}\Omega\text{cm}^2$  measured at 10 Hz, which is an order of magnitude lower than that of commercially available material (e.g., Ten20 paste). Furthermore, the incorporation of ionic salts, such as NaCl and LiCl, into a hydrogel makes it more conductive.<sup>84</sup> Such hydrogels show not only intrinsic softness and stretchability but also improved chemical and biological compatibility with tissues, making them promising candidate materials for soft bioelectronics.<sup>21</sup>

However, hydrogels with high ionic concentrations can effuse high levels of external ions to surrounding tissues, thereby disturbing the ionic equilibrium of tissues *in vivo* and limiting their use in implantable devices.<sup>32</sup> To resolve this issue, Zhao et al. utilized a two-phase aqueous system made of salt/poly(ethylene glycol) (PEG), in which the salt-containing patterns were safely encapsulated inside the electrically inert PEG hydrogel matrix (Figure 2D).<sup>32</sup> In tests conducted in the tibialis anterior

muscle of rat, this two-phase system effectively prevented the undesirable diffusion of high-concentration ions from the hydrogel into the surrounding tissues while allowing the circuit made of the ion-conductive hydrogel to electrically stimulate the target muscles over a prolonged period.

It is noteworthy that conducting polymers, such as polypyrrole (PPy),<sup>85</sup> polyaniline (PAni),<sup>86</sup> or PEDOT,<sup>87</sup> can be of benefit when used alone or when mixed with hydrogels, as they minimize the electrical differences between a device and the implanted tissue. Conducting polymers can transfer electrons through  $\pi$ -conjugation (delocalized electrons in overlapped pi-orbitals of alternating single and double covalent bonds) and exhibit greater conductivity than do conventional hydrogels.<sup>88</sup> In addition, ions can penetrate into the bulk conducting polymer. This leads to a high volumetric capacitance of the conducting polymer, which significantly lowers the electrical impedance and increases charge-injection capacity compared with that of conventional bioelectronics.<sup>89</sup>

Flexible microelectrode arrays—fabricated by using a conducting polymer, poly(3,4-ethylenedioxythiophene):polystyrene sulfonate (PEDOT:PSS)—offer a high SNR (6.2 dB)<sup>39</sup> and a high charge-injection capacity ( $2.71 \text{ mC cm}^{-2}$ ),<sup>38</sup> enabling safe neural interfaces. PEDOT:PSS is composed of conjugated PEDOT segments, which are hydrophobic. Its hydrophilic segment, PSS, enables PEDOT to be dispersed in an aqueous solution. To increase the conductivity of PEDOT:PSS, the crystallinity of PEDOT can be increased, but this modification makes the PEDOT:PSS film stiff and susceptible to the formation of cracks.<sup>90,91,92,33</sup> To improve the mechanical softness of conducting polymers, such as PEDOT:PSS, a nonvolatile surfactant plasticizer, Triton X-100, is introduced to modify their viscoelastic properties.<sup>33</sup> The resulting material, which can be repeatedly stretched and molded similar to the rubber “playdough” (Figure 2E), exhibits several unique properties, including compatibility with conventional printing techniques, good adhesion onto both hydrophilic and hydrophobic substrates, and mechanical stability (up to 10% stretching). Further improvements of stretchability were achieved by coating the viscoelastic PEDOT:PSS with silicone encapsulations.

Instead of using the plasticizer, composites of a conducting polymer and a hydrogel<sup>88</sup> can be used. The hydrogel enhances softness, while PEDOT:PSS is responsible for conductivity. Thus, the hydrogel-PEDOT:PSS composite offers advantages of both components, a relatively high electronic conductivity and ionic conductivity, and an inherent soft mechanical property, making them a promising material candidate for the soft bioelectronics.<sup>50</sup> Although hydrogel-PEDOT:PSS composite offers reasonable conductivity, their conductivity is still far lower ( $\sim 40 \text{ S/cm}$ <sup>93</sup>) than the conventional metal electrode (e.g.,  $\sim 6.3 \times 10^7 \text{ S cm}^{-1}$  for the silver electrode<sup>94</sup>). Therefore, the conductivity should be improved further.

### Improving Conductivity with Nanomaterials

Introducing nanomaterials other than conducting polymers to hydrogels has proved to be an effective way to improve the conductivity of hydrogel composites. Carbon-based nanomaterials, such as carbon nanotubes (CNTs) and graphene, have gained attention as conductive filler materials for hydrogel composites.<sup>51</sup> In this approach, a conducting hydrogel composite can be fabricated by incorporating CNTs and supra-molecular  $\beta$ -peptide into a hydrogel matrix, for example, to record intracortical and epidural neural signals.<sup>95</sup> In this example, the CNTs formed a 3D electrical percolation network within the hydrogel medium, which facilitates signal transmission. Due to the viscoelastic nature of the hydrogel composite, tight neural/hydrogel contacts were



achieved, enabling the seamless integration of the soft electrodes with the target neural tissues.

One possible way to achieve higher electrical conductivity is to incorporate metallic nanomaterials into the hydrogel.<sup>52,53</sup> For example, Ahn et al. transferred silver nanowires (AgNWs) directly into a polyacrylamide-based hydrogel. This approach achieved the efficient formation of a percolation network due to the high aspect ratio of the NWs, as well as the high intrinsic conductivity of silver, which contributed to a high electrical conductivity while maintaining the soft mechanical properties of the hydrogel (Figure 2F).<sup>34</sup> The microelectrode fabricated using these materials did not show any significant change in resistance even after 100 cycles of the bending test.

Other approaches that embed conductive nanomaterials<sup>96</sup> into elastomeric matrices<sup>79,97,98</sup> have also been reported to improve both the conductivity and stretchability of soft bioelectronics.<sup>57,58</sup> For example, a nanocomposite composed of ligand-exchanged ultra-long AgNWs and a styrene-butadiene-styrene (SBS) thermoplastic elastomer has been reported (Figure 2G).<sup>35</sup> In this study, the polyvinylpyrrolidone ligands that were originally on the surface of the AgNWs were exchanged with hexylamine to disperse the NWs homogeneously in the organic-phase SBS. The resulting nanocomposite exhibited a high conductivity of  $11,210 \text{ S cm}^{-1}$  and, remarkably, softer mechanical properties than those of the original film of the same material when patterned into a serpentine mesh structure. The serpentine mesh electrodes could record electrophysiological signals and apply feedback stimulations on the heart ventricle in a rat model of myocardial infarction.<sup>35</sup>

Because direct exposure to the silver ions that leach from AgNWs can induce adverse health effects, there have been attempts to increase the biocompatibility of the AgNWs by passivating their surface with an inert material, such as gold.<sup>56</sup> Choi et al. coated the surface of the AgNWs with a gold shell, which greatly improved their biocompatibility, as confirmed by enhanced cell viability *in vitro* and reduced fibrotic reactions *in vivo*. These gold-coated AgNWs were embedded in an elastomeric block-copolymer matrix with the assistance of hexylamine-induced phase separation, and the resulting nanocomposite exhibited a high conductivity ( $41,850 \text{ S cm}^{-1}$ ) and excellent stretchability (266%).

In addition to the materials used to create the electrode itself, the materials used to encapsulate an electrode are also important, particularly for long-term monitoring and stimulation. Conventional encapsulation materials such as quartz glass, Teflon, and parlyene have shown high dielectric constants that can minimize stray capacitances. However, they have high moduli, which cause a mechanical mismatch with the brain tissue. Some unconventional approaches for the fabrication of the encapsulation layer have been reported, such as the use of an elastic fluorinated photoresist.<sup>49</sup> An insulating layer consisting of this material was patterned directly onto the electrically conductive hydrogel electrode and exhibited Young's modulus similar to that of soft tissues (<30 kPa). Another example is a cardiac stimulator of the conductive nanocomposite sandwiched between soft insulating SBS layers<sup>56</sup> along the entire device except for the contact pads.

## FABRICATION TECHNIQUES CUSTOMIZED FOR SOFT MATERIALS AND DEVICE DESIGN

While the unconventional soft materials described in the previous section, such as ultra-thin inorganic/metallic membranes, ionic hydrogels, conducting polymers, and metallic elastomeric nanocomposites, show the potential for minimizing the mechanical,

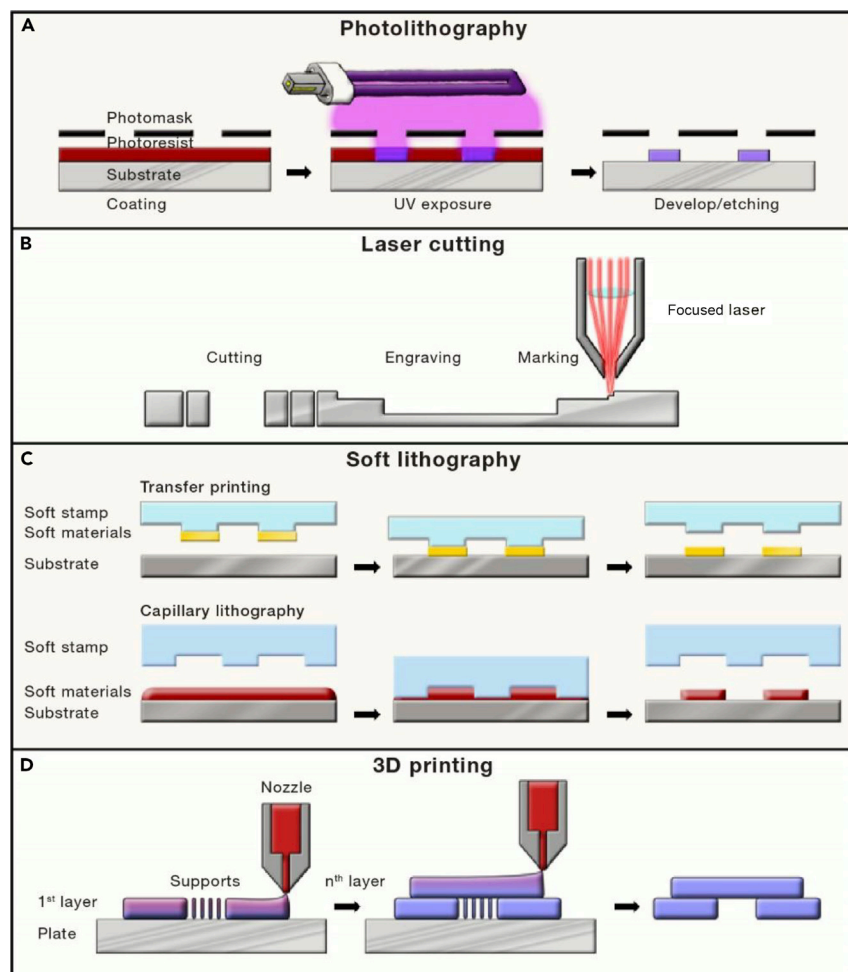


**Figure 3. Novel Processing Techniques for Unconventional Soft Materials**

(A) Schematic of the photolithography process. The photoresist is coated onto the target substrate, followed by UV exposure and the developing step (for ultrathin metal layers).

(B) Schematic of the laser-cutting process. The highly focused laser cuts, engraves, or marks the target substrate (usually conductive polymers or elastomeric nanocomposite) with a high degree of freedom.

(C) Schematic of different soft lithography processes: transfer printing (top) and capillary force lithography (bottom) (used for hydrogels, conductive polymers, and elastomeric nanocomposites).

(D) Schematic of the 3D-printing process. The polymeric ink is deposited from the nozzle in a layer-by-layer manner (some hydrogels, conductive polymers, and elastomeric nanocomposites were used as an ink).

chemical, and electrical differences between the biotic and abiotic systems, their successful application to bioelectronics requires high-precision material processing and assembly techniques. However, the characteristics of unconventional soft materials, such as weak resistance to organic solvents, high porosity, and high water content,<sup>99</sup> limit the use of fabrication methods that involve chemicals and high-temperature processes. In this section, we discuss the patterning and assembly techniques that are being customized to fabricate soft bioelectronic devices using unconventional soft materials.

Photolithography is a representative patterning technique that transfers an original pattern onto a photomask to a target substrate (Figure 3A).<sup>100</sup> In this approach, a

light-sensitive polymeric solution, known as the photoresist, is coated onto a target substrate, in which the photomask is irradiated using UV light. After developing the photoresist in a basic solution, the material underneath the photoresist can be patterned using chemical wet etching or physical dry etching.<sup>101</sup> Because photolithography requires the use of various organic solvents and solutions, only materials with high resistivity to organic solvents, such as ultrathin metallic membranes, can be used. Despite the limited compatibility of photolithography to selected materials, the photolithography technique is a powerful method to use for fabricating high-density electrode arrays. For example, a high-density, 360-channel, flexible active electrode array has been fabricated using photolithography with an electrode size and inter-electrode spacing of  $300 \times 300 \mu\text{m}$  and  $500 \mu\text{m}$ , respectively.<sup>102</sup>

Normally, photolithography cannot be applied to soft materials such as hydrogels due to their material properties (e.g., high water content, low chemical resistance against organic solvents). However, through careful manipulation of the chemical characteristics of the hydrogel and judicious design of the fabrication process, several hydrogels have been found to be compatible with the photolithography process.<sup>103</sup> For example, a micropatterned electrically conductive hydrogel (ECH) on a fluorinated elastic substrate, dimethacrylate-functionalized perfluoropolyether (PFPE-DMA), has been created via a two-step process.<sup>49</sup> In the first step, an ion gel was prepared by blending an ionic liquid (4-(3-butyl-1-imidazolium)-1-butananesulfonic acid triflate) with a conducting polymer (PEDOT:PSS). The formation of a gel using an ionic liquid instead of water was crucial for the patterning because the high water content of most hydrogels prevents their application to photolithography. In the second step, after patterning the ion gel on the PFPE-DMA substrate, the ionic liquid was removed via water exchange to transform the gel into a patterned ECH, which could work as an electrode for low-voltage neural stimulation. Although photolithography could be successfully used for this particular type of hydrogel, most hydrogels cannot satisfy the harsh conditions required for photolithography.

Laser-cutting techniques provide a way around some of the obstacles associated with photolithography and employ a well-focused laser to pattern the target material into the desired geometry (Figure 3B).<sup>104,105</sup> Polymeric films, including those with low chemical resistance, can be rapidly sliced, engraved,<sup>106</sup> or marked on a large scale without sacrificing their intrinsic electrical and chemical properties.<sup>107</sup> As an example, Henle et al. created a micro-ECoG array composed of polydimethylsiloxane (PDMS) and platinum. PDMS is an elastomer that is incompatible with the photolithographic process because the organic solvents commonly used in photolithography, such as acetone and 1-propanol, diffuse into the polymeric matrix, causing it to swell.<sup>108</sup> Therefore, the authors took a laser-based manufacturing route to pattern PDMS into a microelectrode array of  $2 \times 4$  electrodes with an inter-electrode distance of  $0.95 \text{ mm}$ . As the electrode was fabricated using medical-grade soft silicone rubber, long-term subdural implantation into the rat cerebral cortex (up to 18 weeks) was possible.

Although the laser-cutting method is simple, rapid, and applicable to a wide variety of materials, its spatial resolution is in the range of a few hundreds of micrometers.<sup>109</sup> This resolution is rather poor in comparison with photolithography, which shows a resolution of  $\sim 100 \text{ nm}$  with UV light and promises future improvement through the use of electron beams and X-rays.<sup>110</sup> Moreover, the heat generated during the laser-cutting process can break down the weak internal bonds of soft materials.

Soft lithography is a method that takes advantage of both laser-cutting and photolithography,<sup>111,112</sup> such as a wide selection of materials, a high patterning resolution,

and mild fabrication conditions (Figure 3C).<sup>113,114</sup> Its mechanism relies on the use of replicating stamps<sup>115</sup> or molds<sup>116</sup> that are fabricated by using photolithography or other high-resolution patterning methods.<sup>117,118</sup> Using this approach, electrodes can be economically fabricated with high resolution.<sup>119</sup> The serpentine-mesh-shape AgNW/SBS nanocomposite<sup>120</sup> developed by Park et al. described in the previous section is one such example.<sup>35</sup> Because the SBS substrate is easily dissolved in organic solvents, such as toluene, a soft lithography method that uses pre-fabricated molds can offer an efficient device fabrication strategy.

Printing techniques, such as screen printing and inkjet printing, can also be used to fabricate soft bioelectronics. Screen printing is a technique whereby a pre-patterned screen is used to transfer a patterned ink onto a substrate through the screen. A blade moves the ink across the screen to fill the open region of the screen. Mineev et al. have utilized the screen-printing method to fabricate a soft neural implant, the shape and elasticity of which was designed to be similar to that of the dura mater, a so-called e-dura.<sup>121</sup> Inkjet printing is another promising fabrication method. For instance, Adly et al. fabricated a microelectrode array on various substrates using the inkjet-printing method.<sup>122</sup> In this study, feedlines (silver), electrodes (carbon), and encapsulation layers (polyimide) were printed in a layer-by-layer manner onto various substrates, such as PDMS, agarose, and gelatin.

3D printing has also been recently used to fabricate complex structures that can mimic biological conditions.<sup>123</sup> 3D printing is an additive process whereby an object is created by piling up successive layers of materials (Figure 3D). Consequently, 3D printing can produce complicated shapes using fewer amounts of materials, which is a marked difference from the previously described methods that rely on cutting bulk-state materials.<sup>124</sup> However, typical solution-phase electronic materials, such as conventional conducting polymers (e.g., PEDOT:PSS, PPy), are not viscous enough to be used in 3D printing.<sup>125,126</sup> Yuk et al. tackled this problem by developing a 3D-printable conducting ink based on PEDOT:PSS.<sup>127</sup> In this work, they developed PEDOT:PSS suspensions with an appropriate viscosity for 3D printing through the controlled redispersion of lyophilized polymer nanofibrils. The printability of the resulting conducting polymer ink allowed various 3D structures to be fabricated with high resolution (~30  $\mu\text{m}$ ) and with a high aspect ratio (over 20 layers). Furthermore, because 3D printing shares a similar processing step with conventional inkjet printing, a 2D soft neural probe capable of recording local field potentials from a mouse brain was fabricated through continuous printing. The fabricated neural probe was used to record local field potential (LFP) and extracellular action potentials in a freely moving mouse.<sup>127</sup>

Although each fabrication technique discussed above has unique characteristics and advantages, techniques besides photolithography are seldom used commercially. This is mainly due to the two difficulties; low yield of the processes (quality control is more difficult than photolithography) and their incompatibility with the commercialized input and/or output instruments. However, bioelectronics fabricated with soft materials and their uniquely customized fabrication techniques are widely studied in academic research labs and are providing valuable information discussed in the following section.

## USING SOFT NEUROBIOELECTRONICS FOR ELECTROPHYSIOLOGICAL RECORDINGS

EEG, ECoG, and ICE are major electrophysiological signal recording techniques (Figure 4A) that employ electrodes optimized for each technique and that integrate with

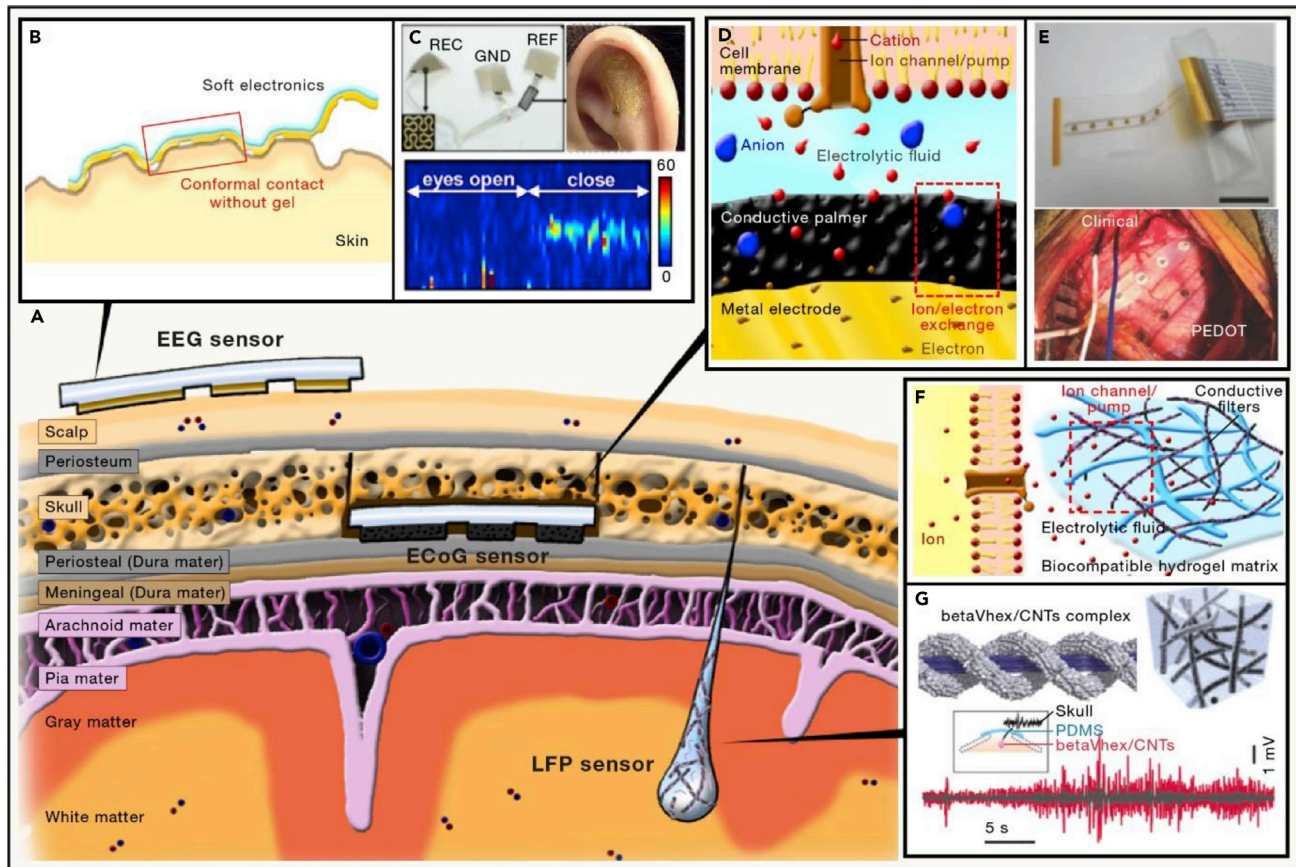


**Figure 4. Soft Bioelectronics for Electrophysiological Recordings**

(A) Schematic of soft unconventional electronic devices on various recording sites in the brain: EEG sensors located on the scalp, ECoG sensors located on the dura mater under the skull, and ICE sensors located in the subcortical area.

(B) In this example of an EEG sensor, an ultrathin metal electrode on a highly flexible polymer substrate can make conformal contact with the curvy rough skin without an electrolytic gel.

(C) Image of a representative EEG sensor made of an ultrathin metal layer on a flexible substrate, including recording (REC), ground (GND), and reference (REF) electrodes (top left). Optical image of an electrode placed on the auricle (top right). EEG signals recorded using ultrathin EEG sensors (bottom). Reproduced with permission.<sup>133</sup> Copyright 2015, National Academy of Sciences

(D) Schematic of a conductive polymer that can reduce the electrical mismatch between tissue and device by ion/electron exchange.

(E) Image of the PEDOT:PSS-based ECoG sensor (top: scale bar, 3 cm) and its application on the human cortex (bottom). Reproduced with permission.<sup>39</sup> Copyright 2018, Wiley-VCH.

(F) Schematic of a composite of a hydrogel and nanomaterials, which minimizes the electrical and chemical mismatch between tissue and the device.

(G) Schematic of the building blocks of the betaVhex/CNT complex (top left) and its hydrogel composite (top right). ICE signals recorded by an electrode made of the hydrogel composite (bottom). ICE recorded by the hydrogel composite (red) and ICE recorded by the bare hydrogel (gray). The inset illustrates implantation of the composite into the skull. The open area was covered by PDMS. Reproduced with permission.<sup>95</sup> Copyright 2020, American Chemical Society.

different target tissues depending on the type of the signal recorded,<sup>128</sup> such as on the scalp for EEG,<sup>129</sup> on or under the dura mater for ECoG,<sup>130</sup> and in the intracortical area for ICE.<sup>131</sup> Each recording method has its advantages and disadvantages in terms of its signal amplitude, spatiotemporal resolution, and invasiveness. EEG has low amplitude and low resolution, but its invasiveness is also low. ICE (which includes LFP, intracortical EEG, and single-unit/multi-unit recordings) has high amplitude and high resolution, but its invasiveness is also high. ECoG sits in the middle of EEG and ICE in terms of its amplitude, resolution, and invasiveness. When the distance between the electrode and target neuron increases, the amplitude of the extracellular potential decreases. It is challenging to filter a signal with low amplitude (e.g., EEG) from its surrounding noise. Therefore, the

recording methods that are more invasive (such as intracortical recording) can provide more informative signals with a higher SNR.<sup>132</sup>

Soft bioelectronics, fabricated using the aforementioned unconventional soft materials, have contributed to advances in these electrophysiological recording techniques—particularly for long-term, high-quality neural signal recordings—by resolving mechanical, chemical, and electrical mismatches between the brain tissue and the device,<sup>134</sup> as we discuss below.

An EEG sensor is used to record electrophysiological signals induced by brain activities on the scalp.<sup>135</sup> This on-skin recording method of brain signals has a particular advantage over other recording methods due to its non-invasiveness. However, in this technique brain waves are recorded after passing through multiple tissue layers. Therefore, EEG signals show unspecified low amplitudes (5–300  $\mu\text{V}$ ) and low spatio-temporal resolutions ( $\sim 10$  mm,  $\sim 50$  ms). To maximize the SNR by minimizing the impedance, an electrolytic gel is often used.<sup>136</sup> However, this gel typically dries out after a fixed amount of time and the signal quality deteriorates. As a result, novel, soft, skin-mountable recording electrodes that achieve high SNRs without the use of electrolytic gel have been developed,<sup>137</sup> which provide low impedance and a high level of comfort (Figure 4B).<sup>138,139,140</sup>

One example of a novel soft electrode is that developed by Norton et al., which has fractal geometries and consists of ultrathin gold electrodes patterned onto an elastomeric film.<sup>133</sup> This ultrathin electrode could be conformally mounted onto the auricle and mastoid bone of a human subject, where long-term, high-fidelity EEG recordings were gathered without the use of electrolytic gels (Figure 4C). The electrode was patterned into the serpentine-shape space-filling curve, resulting in an effective modulus of  $\sim 130$  kPa, which enables conformal contact on the skin. All of the materials used in this system, such as silicon, gold, and polyimide, are biocompatible. Keratinocyte cells cultured on this device also showed high cell viability (70.0%), indicating its low cytotoxicity. Because of the high flexibility and system-level softness of this device, the reference and ground electrodes could be mounted onto the curvy auricle of the human ear, enabling the mechanical and electrical noise of the recording electrode on the skin to be isolated. Moreover, users did not feel any notable skin irritation or discomfort due to the device's flexibility, softness, and biocompatibility, which is crucial for achieving long-term recordings with high comfort. Indeed, volunteers were able to wear the device for more than 2 weeks during their daily life, enabling their EEG alpha rhythm to be successfully recorded in the laboratory during this time. Moreover, the soft, skin-conformal electrode was used to record steady-state visually evoked potentials (SSVEP) and the P300 wave for brain-computer interface applications, which enabled the volunteers to type the word "computer" with high accuracy (84%) using the recorded EEG signals and the SSVEP-based text speller program.

ECoG monitoring, which measures electrophysiological signals on the dura mater,<sup>141</sup> requires electrodes that have higher biocompatibility and mechanical softness than EEG sensors<sup>142</sup> because they directly contact the brain surface.<sup>64,102</sup> Higher spatiotemporal resolutions ( $\sim 1$  mm,  $\sim 30$  ms), higher amplitudes (10  $\mu\text{V}$  to mV), and higher SNRs can be obtained from ECoG relative to scalp EEG. In one example of ECoG monitoring, neural signals recorded on the brain surface were obtained using soft electrodes made of patternable organic materials (Figure 4D).<sup>143,144</sup> PEDOT:PSS-based high-SNR ECoG sensors have also been tested in human cognition studies ( $n = 3$  patients visual/vocal tasks) and in a clinical setting

( $n = 1$  patient during an epileptic seizure) (Figure 4E).<sup>39</sup> The electrochemical results show that PEDOT:PSS electrodes had a higher SNR than did conventional platinum electrodes (an order of magnitude lower, in terms of noise density) across all frequency bands. Also, in recording tests with human subjects, the PEDOT:PSS electrodes produced a higher-quality ECoG signal relative to platinum macrodot electrodes. These results show the possibilities of using PEDOT:PSS electrodes in clinical settings.

The ICE monitoring technique records intracortical electrophysiological signals that feature higher SNRs and contain more localized information (spatiotemporal resolution of  $\sim 0.1$  mm and 30 ms) than do EEG and/or ECoG signals.<sup>145,146</sup> Although ICE recordings have particular benefits, the widespread use of ICE sensors, except in a clinical setting, is limited due to its invasive nature.<sup>147,9</sup> Moreover, the soft and ion-rich fluidic characteristics of the intracortical environment make the long-term application of conventional, rigid bioelectronics to ICE recordings challenging because of the mechanical, chemical, and electrical mismatches.<sup>46</sup> Additionally, even novel materials have drawbacks in meeting the strict criteria for ICE sensors. For example, thin metal films have high conductivity and can be fabricated into high-resolution electrodes<sup>134,148</sup> but are chemically and electrically incompatible with the intracortical environment.<sup>9</sup> Moreover, while conductive polymers and hydrogels can be mechanically and chemically compatible with this environment, they show low conductivity.

To address these challenges, two or more materials are sometimes combined to compensate for the disadvantages of the other in order to minimize mismatches without sacrificing functional advantages (Figure 4F).<sup>145,48,146</sup> In one example, Nam et al. fabricated a syringe-injectable ICE electrode with a composite of a supramolecular  $\beta$ -peptide-based hydrogel and a conductive filler of carbon nanotubes (CNTs) that could mechanically and chemically mimic the brain tissue. The resulting betaVhex/CNT/hydrogel composite shows a low modulus of  $\sim 1,500$  Pa, which is similar to that of brain tissue and thus can reduce mechanical damage.<sup>95</sup> Normally, ICE electrodes must be stiff enough to penetrate the brain tissue during their initial insertion into the cortex, but they should also be soft enough to prevent mechanical damage to the cortex. This causes a serious dilemma when designing and fabricating ICE sensors. Although the hydrogel composite is as soft as the brain tissue, the hydrogel composite-based ICE sensor can be implanted into the targeted area by injection through a syringe. In the study by Nam et al., the injectable device was implanted into the II/III layer of the somatosensory cortex of the chronic epileptic mouse model. The large surface area of the composite, the ionic interface of the hydrogel, and the high conductivity of the CNT significantly reduced the impedance of the sensor (Figure 4G), and the electrode provided high-quality ICE recordings. Specifically, the signal intensities of the beta and gamma bands during the epileptic event were 3-fold and 2.4-fold higher than those obtained by using a normal, bare hydrogel electrode and a bare electrode, respectively. Although the morphology of the hydrogel composite electrode was significantly altered due to its flexibility, it was only slightly degraded due to the high stability of  $\beta$ -peptide, with no interference to cerebral blood flow. Histologically, the hydrogel electrode showed significantly lower inflammatory responses after 12 weeks of implantation relative to a conventional metal electrode.

The choice of a particular soft bioelectronic device ultimately depends on the requirements of its specific application. However, there are some general principles to observe, as follows. EEG sensors need to be soft for conformal contact and to have low impedance to achieve a high SNR. ECoG sensors need to have high resolution (thus the materials used to create them need to be compatible with high-

resolution patterning) and should be soft and non-toxic to minimize chronic immune responses. ICE sensors must be very small (submillimeter scale for animals) to reduce mechanical damage, non-toxic to minimize immune responses, and chemically inert to minimize material degradation. Additional considerations should be made according to specific research targets and requirements. The aforementioned recording techniques have been combined with modulation technologies to deliver electric current, and/or optical stimulation and chemical drug delivery, to constitute integrated monitoring and feedback modulation systems. Some of these representative therapeutic trials are introduced in the next section.

### OPPORTUNITIES FOR TREATING NEUROLOGICAL DISEASE WITH NOVEL SOFT BIOELECTRONICS

Although conventional electrotherapies and/or chemotherapies have contributed significantly to the treatment of various neural diseases, such as Parkinson's disease, epilepsy, chronic pain, and brain tumors, there is still room to improve on the therapeutic efficacy of these treatments, which newly emerging soft bioelectronic approaches aim to achieve (Figure 5A).<sup>149</sup> For example, soft bioelectronic approaches can provide more effective electrical stimulations than can conventional rigid devices owing to lowered contact impedance, enhanced charge-injection capacity, and suppressed generation of insulative scar tissues.<sup>150,151</sup> Additionally, unconventional materials used in advanced soft chemotherapeutic electronics can release drugs directly into a target region in a controllable, programmable, and localized manner, while reducing mechanical tissue damage and the side effects of conventional chemotherapies (Figure 5A).

Unconventional soft bioelectronics has shown promise for use in advanced electrotherapies, which can play an important role in the regulation or enhancement of specific neural activities via electrical stimulation. For example, a soft neural interfacing device that mimics the shape and mechanical property of the dura mater has been reported (Figure 5B).<sup>121</sup> The soft silicone substrate of this implant, named e-dura, was developed to minimize mechanical mismatch between the device and brain tissue while maintaining stable electrical conductivities using stretchable gold interconnects. The soft electrodes coated with the platinum-silicone composite also contributed to minimizing chemical and electrical mismatches. In their study, Minev et al. demonstrated the potential of e-dura as a biocompatible, long-term electrical stimulator for rat spinal cord, by comparing its long-term biocompatibility with that of conventional flexible neural signal recording electrodes made of a thin metal film on a polyimide substrate. Although the soft e-dura material was much thicker (~100  $\mu\text{m}$ ) than the thin polyimide-based electrode (~25  $\mu\text{m}$ ), the deformation of spinal neural tissue after 6 weeks of e-dura implantation in a healthy rat was much smaller relative to that produced by the polyimide-based electrode, without notable differences from the controls (sham-treated spine), due to the mechanical softness of the e-dura. These researchers also implanted an e-dura into lumbosacral segments of a rat with permanent paralysis of both legs due to spinal injuries. The electrical stimulation provided by the e-dura enabled the paralyzed rat to walk and mediated reliable therapeutic effects during 6 weeks of the rehabilitation period. In a later study, the e-dura was combined with a computed protocol that reproduced natural motor neuron activation during locomotion. The electrode design and the spatiotemporal stimulation pattern were determined after monitoring spatiotemporal activation patterns in healthy rats. The spatiotemporal neuromodulation provided via e-dura improved the overall locomotion quality, including weight-bearing capacity (25%–60%) and locomotion duration (40%–270%) in paralyzed adult rats in comparison with those provided with continuous modulation.<sup>155</sup>



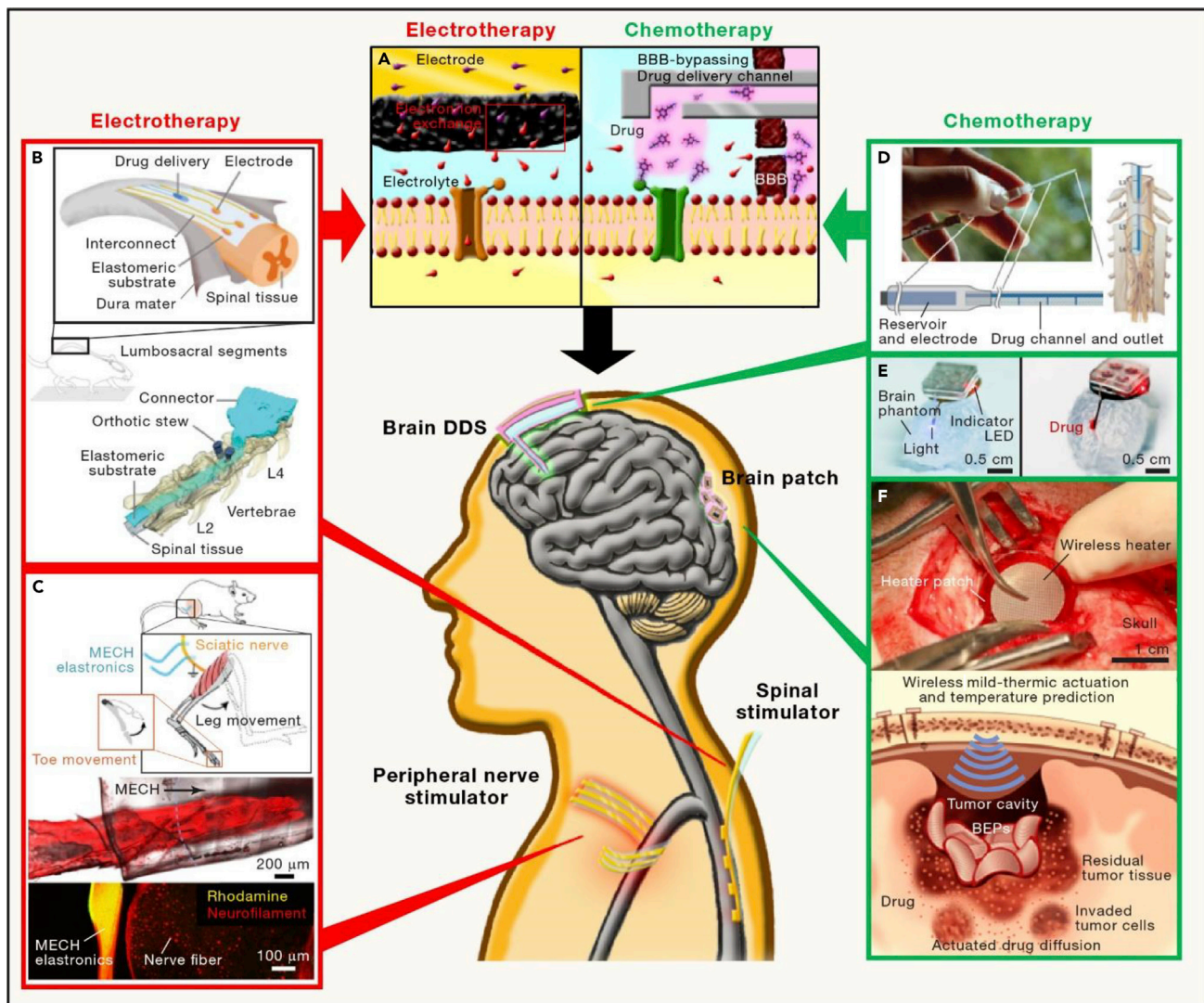


**Figure 5. Soft Bioelectronics for Electrical and Chemical Therapy**

Schematics showing examples of the therapeutic applications of soft bioelectronics.

(A) Soft unconventional materials can support electrotherapy via ion/electron exchange and chemotherapy by enabling local drug delivery. The soft drug-delivery channel (gray layer) can deliver drugs directly to target cells, bypassing the blood-brain barrier (BBB) (shaded brown), which prevents drug molecules from infiltrating the extracellular fluids.

(B) Schematic of the e-dura implanted into the lumbosacral segments of a model animal that has permanent paralysis of both legs due to spinal injuries. Reproduced with permission.<sup>121</sup> Copyright 2015, AAAS.

(C) Schematic of the micropatterned electrically conductive hydrogels (MECH) implanted into the sciatic nerve of a mouse to enable peripheral nerve stimulations (top). Microscopic image showing MECH electronics mounted on the sciatic nerve and its cross-sectional image (bottom). Reproduced with permission.<sup>49</sup> Copyright 2019, Springer Nature.

(D) PEDOT:PSS-based electronics that can precisely deliver drugs to reduce pain (left). Schematic illustration describing drug-delivery device implanted in the spine (right). Reproduced with permission.<sup>152</sup> Copyright 2015, AAAS.

(E) Photographs of the battery-free, injectable optical (left) and chemical (right) brain stimulator on the brain phantom (i.e., artificial brain tissue made of 0.6% agarose gel). Reproduced with permission.<sup>153</sup> Copyright 2019, National Academy of Sciences

(F) Optical image (top) and schematic illustration (bottom) of the flexible, biodegradable, and sticky wireless drug-delivery device used to treat brain tumors. Reproduced with permission.<sup>154</sup> Copyright 2019, Springer Nature.

Soft bioelectronic devices can also be implanted on the peripheral nerve to perform neuromodulation.<sup>156</sup> For example, a conductive-hydrogel-based microelectronic, which was fabricated by mixing conductive polymer (PEDOT:PSS) with the hydrogel

matrix, has been used to provide low-voltage neuromodulation (Figure 5C).<sup>49</sup> Owing to the low electrical impedance ( $\sim 1$  k $\Omega$ ), this microelectronic device exhibited high current-injection density ( $\sim 30$  times higher than platinum electrode), high conductivity ( $\sim 50$  S cm<sup>-1</sup>), and stable electrical performance even under external strain. When implanted on the sciatic nerve of anesthetized mice, the electrodes delivered a high excitation current density of 10 mA cm<sup>-2</sup> at a low voltage of 50 mV for neuromodulation. The implanted electrodes maintained intimate contact with the sciatic nerves—even during the repetitive leg movement of the subject animal—due to their low Young's modulus ( $\sim 30$  kPa) and high elasticity. Furthermore, the microelectrodes could deliver localized stimulations to the peripheral nerve bundles and could control precise toe movements by adjusting the stimulation frequency.

The use of electrical stimulation for diagnosis and real-time feedback therapy is of clinical relevance not only for the nervous system but also for other organs that are controlled by electrophysiological signals, such as the heart,<sup>13,157</sup> stomach,<sup>158</sup> muscle,<sup>159</sup> and endocrine organs.<sup>160,148</sup> For example, an epicardial mesh based on a nanocomposite composed of highly conductive AgNWs and an elastomer (SBS) has been fabricated.<sup>35</sup> When implanted in a rat heart, this epicardial mesh can detect abnormal electrical activities, such as ventricular tachycardia and ventricular fibrillation, in a freely moving rat.<sup>35</sup> Furthermore, its electrical conductivity was sufficiently high to deliver a synchronized electrical stimulation to the ventricles of a rat with myocardial infarction.<sup>59</sup> These results show that epicardial mesh electronics can thus modulate a diseased heart, including heartbeat control and defibrillation, without interfering with normal cardiac contraction.

Chemotherapies have long been used in the clinic to treat various neural diseases.<sup>161</sup> However, the typical administration routes available for these therapies, including oral administration or intravenous injection, often fail to deliver the desired amount of a drug to the target brain sites, principally because they deliver a drug to the entire circulation system and the drugs fail to cross the blood-brain barrier (BBB). In addition, drugs that spread non-specifically to other organs can cause side effects.<sup>162</sup> To avoid these issues, many researchers have attempted to develop local drug-delivery systems (DDS) with which to control chemotherapy doses at the desired site while minimizing side effects.<sup>163,164</sup> However, conventional DDS tend to have rigid properties and thus are mechanically mismatched with brain tissues.<sup>165,166</sup> As an alternative, soft bioelectronics can provide effective, controllable, and long-term chemotherapy to neural tissues.<sup>167</sup> Moreover, intracranial soft DDS enable drugs to be delivered directly to extracellular fluids, thus bypassing the BBB and increasing drug efficacy.<sup>168</sup>

In another example, an implantable, organic bioelectronic device that locally delivers therapeutics in an electrically controlled manner has been used to treat chronic pain (Figure 5D).<sup>152</sup> This PEDOT:PSS-based implantable device under applied electrical current delivers therapeutics to a neuropathic pain model. When voltage is applied to an electrode, the PEDOT:PSS electrode is oxidized and, thus, the PEDOT:PSS counter electrode is reduced. When the electrodes are overoxidized a salt bridge forms through the cation-selective channel, enabling the unidirectional electrophoretic transport of cations (therapeutics) out of the reservoir. The device tip was 1.2 mm wide, 40 mm in length, and 0.2 mm thick, which is suitable for spinal cord implantation. To test this device, it was implanted onto the spinal cord of rats with nerve injury, and inhibitory neurotransmitter  $\gamma$ -aminobutyric acid (GABA) was locally delivered. A significant decrease in pain was observed at a low dosage but without side effects. The positive control group with GABA<sup>+</sup> delivery showed

improved withdrawal thresholds ( $\sim 140$  mN) while the negative control group with  $H^+$  delivery showed low withdrawal thresholds ( $\sim 40$  mN), which verifies the device's therapeutic effects. The high mechanical compatibility of the soft device with the surrounding tissue minimized potential side effects. This result shows the potential for using a soft and implantable spinal DDS to control chronic pain.

In another example, a battery-free injectable microsystem was developed that can deliver both chemical drugs and optogenetic stimulations to the brain (Figure 5E).<sup>153</sup> This system consists of a soft microfluidic channel and a light-emitting probe, which was implanted into the brain and connected to a miniaturized exterior unit that includes a control circuit, a power-harvesting coil, and a drug reservoir. The DDS was made of PDMS and had a cross-sectional area of  $0.035 \text{ mm}^2$ , which is much smaller than that of conventional 26-gauge metal cannulas ( $0.166 \text{ mm}^2$ ). The device could deliver the drug solution through the microfluidic channel at a rate of  $\sim 2 \mu\text{L min}^{-1}$  up to a volume of  $3.92 \text{ mm}^3$ . The system could also manipulate neural activity in the deep brain (ventral tegmental area of brainstem and hippocampus) of freely moving mice in a locomotor activity test. The design of this device also offered the possibility of separate or concomitant pharmacological and optogenetic manipulations in a region-specific, spatially overlapping, and minimally invasive manner. The soft characteristics of the device also minimized the mechanical mismatch between the implant and the tissue, and reduced lesion and immunoreactive glial responses were observed even after long-term implantation (lesion size of  $\sim 8 \times 10^4 \mu\text{m}^2$ ), relative to that seen for conventional metal cannulas (lesion size of  $\sim 20 \times 10^4 \mu\text{m}^2$ ).

Recently, a flexible, sticky, and biodegradable wireless device made with ultrathin metal, integrated with a polymer drug reservoir for treating brain tumors, has been reported (Figure 5F).<sup>154</sup> The two sides of this device, a bioresorbable electronic patch, have different surface properties: one side consists of a flexible, hydrophilic oxidized starch patch and the other side consists of a hydrophobic encapsulation. The hydrophilic side shows conformal adhesion to the target brain tissue and allows local drug delivery while the hydrophobic layer exposed to the cerebrospinal fluid minimizes unwanted drug leakage to the fluid. Upon wireless mild-thermic actuation by the external magnetic field, the drugs loaded in the patch are intracranially released with an enhanced drug-diffusion length. The device exhibited a hydrolytic biodegradation period of 10 weeks in the canine brain *in vivo*. The softness of the patch minimized mechanical damage to the brain tissue, thereby preventing neurological side effects. The effectiveness of the device was also confirmed in mouse subcutaneous and canine brain glioblastoma models *in vivo*. In each model, tumors were successfully suppressed ( $p = 0.0048$ ) and survival rates improved ( $p = 0.013$ ) significantly, compared with the control wafer, whose composition is similar to that of the commercialized Gliadel Wafer, within the observation period of 70 days.

## SUMMARY AND FUTURE DIRECTIONS

Soft bioelectronics based on unconventional materials, customized fabrication processes, and novel device designs have brought significant advances to neuroscience and neuroengineering. Key strategies adopted in the development of this area of bioelectronics have focused on reducing the mechanical, chemical, and electrical mismatches between biotic and abiotic systems, and have been successfully used to create recording electrodes and electrical/chemical stimulators that can target the nervous system. These soft devices have also been shown to perform their designated functions inside the nervous system over long time periods without causing

serious mechanical and/or biological damage to implanted tissue. As a sign of their promise, these strategies have been adopted by several leading companies, such as Neuronexus technologies,<sup>169</sup> Neuralink,<sup>170</sup> and Neurolux,<sup>171</sup> to develop soft forms of bioelectronic devices. However, several hurdles remain to be overcome before fully realizing the commercialization and clinical translation of these devices.

First, the uniform, reliable, and reproducible performance of soft bioelectronics between devices must be guaranteed. Unlike conventional silicon/metal-based electronics, the mass-fabrication of soft bioelectronics and packaging process with uniform quality and performance remains quite difficult to achieve due to the unconventional soft and fluidic characteristics of the materials and fabrication processes customized for such materials.

Second, the fabrication of devices with smaller feature sizes and higher resolutions remains challenging. Current fabrication techniques, such as the microelectromechanical system technique, might not be fully compatible with the fabrication of high-density bioelectronics based on soft materials. Further development of high-resolution patterning is needed for the fabrication of such high-density soft bioelectronics.

Third, while smaller electrodes that offer higher resolution enable localized measurements of neural signals, their small dimensions can cause their soft materials to rapidly degrade *in vivo* and might decrease the lifetime of the device. Technical advances are thus needed to produce encapsulation materials that have low fluid permeability and high resistivity, but which can maintain mechanical softness.

Fourth, we require a convenient but safe technique to implant devices with a high spatial resolution. The implant must be sufficiently stiff to support easy handling and accurate placement in the targeted region. Paradoxically, the implant must also be soft enough to prevent tissue damage once implanted. Many research groups have reported new strategies to deal with this paradox, but more sophisticated modulus control techniques and surgical implantation techniques are required.

Fifth, soft devices must be fully biocompatible, highly stable, and non-toxic. Although soft materials have been shown to be highly biocompatible, inflammatory reactions to foreign materials and device biodegradation inside the body remain ongoing issues. Several strategies, such as delivering anti-inflammatory molecules and developing stable and safe encapsulation, offer possible ways to overcome these issues.

Sixth, the size of the bioelectronics must be scaled up from an animal-scale device to a human-scale device. Also, the human-scale device needs to satisfy higher functional thresholds. Because functional effectiveness and biocompatibility might be different between animals and humans, the materials, fabrication processes, and application protocols must be reset for clinical translation. Collaborative work between engineers and clinicians will help to reduce the gap between engineering strategies and medical requirements.

Finally, further integration of individual device components, including sensors, actuators, drug-delivery units, light-emitting devices, power supply, and data transmission, is needed. Devices for recording and therapy are useful alone, but an integrated system can be more beneficial in terms of building a closed-loop system. With such an integrated system, real-time monitoring and controlled feedback

treatment in a wireless manner can be achieved. The soft nature of such a system will allow for both long-term biocompatibility and reliability.

We hope that this review of the approaches being used to develop novel unconventional materials and soft bioelectronic devices will provide a platform that inspires further innovations. Such research, its development, and its applications could indeed change the current clinical paradigm for treating neurological disorders and disease.

## ACKNOWLEDGMENTS

This work was supported by the Institute for Basic Science (IBS-R006-D1 and IBS-R006-A1), Republic of Korea.

## REFERENCES

- Levy, M.N., and Martin, P.J. (1989). Autonomic neural control of cardiac function. In *Physiology and Pathophysiology of the Heart*, N. Sperelakis, ed. (Kluwer Academic Publishers), pp. 361–379.
- Houk, J.C., and Rymer, W.Z. (2011). Neural control of muscle length and tension. In *Comprehensive Physiology Supplement 2. Handbook of Physiology. The Nervous System, Motor Control* (Wiley). <https://doi.org/10.1002/cphy.cp010208>.
- Browning, K.N., and Travagli, R.A. (2014). Central nervous system control of gastrointestinal motility and secretion and modulation of gastrointestinal functions. *Compr. Physiol.* **4**, 1339–1368.
- Ulrich-Lai, Y.M., and Herman, J.P. (2009). Neural regulation of endocrine and autonomic stress responses. *Nat. Rev. Neurosci.* **10**, 397–409.
- Chen, Y., Zhang, Y., Liang, Z., Cao, Y., Han, Z., and Feng, X. (2020). Flexible inorganic bioelectronics. *Npj Flex. Electron.* **4**, 2.
- Shi, Z., Zheng, F., Zhou, Z., Li, M., Fan, Z., Ye, H., Zhang, S., Xiao, T., Chen, L., Tao, T.H., et al. (2019). Silk-enabled conformal multifunctional bioelectronics for investigation of spatiotemporal epileptiform activities and multimodal neural encoding/decoding. *Adv. Sci.* **6**, 1801617.
- Vomero, M., Gueli, C., Zucchini, E., Fadiga, L., Erhardt, J.B., Sharma, S., and Stieglitz, T. (2020). Flexible bioelectronic devices based on micropatterned monolithic carbon fiber mats. *Adv. Mater. Technol.* **5**, 1900713.
- Maynard, E.M., Nordhausen, C.T., and Normann, R.A. (1997). The Utah intracortical electrode array: a recording structure for potential brain-computer interfaces. *Electroencephalogr. Clin. Neurophysiol.* **102**, 228–239.
- Szostak, K.M., Grand, L., and Constantinou, T.G. (2017). Neural interfaces for intracortical recording: requirements, fabrication methods, and characteristics. *Front. Neurosci.* **11**, 665.
- Kim, T.-I., McCall, J.G., Jung, Y.H., Huang, X., Siuda, E.R., Li, Y., Song, J., Song, Y.M., Pao, H.A., Kim, R.H., et al. (2013). Injectable, cellular-scale optoelectronics with applications for wireless optogenetics. *Science* **340**, 211–216.
- Chen, R., Romero, G., Christiansen, M.G., Mohr, A., and Anikeeva, P. (2015). Wireless magnetothermal deep brain stimulation. *Science* **347**, 1477–1480.
- Gutruf, P., Krishnamurthi, V., Vázquez-Guardado, A., Xie, Z., Banks, A., Su, C.J., Xu, Y., Haney, C.R., Waters, E.A., Kandela, I., et al. (2018). Fully implantable optoelectronic systems for battery-free, multimodal operation in neuroscience research. *Nat. Electron.* **1**, 652–660.
- Hong, Y.J., Jeong, H., Cho, K.W., Lu, N., and Kim, D.H. (2019). Wearable and implantable devices for cardiovascular healthcare: from monitoring to therapy based on flexible and stretchable electronics. *Adv. Funct. Mater.* **29**, 1808247.
- Butson, C.R., and McIntyre, C.C. (2005). Tissue and electrode capacitance reduce neural activation volumes during deep brain stimulation. *Clin. Neurophysiol.* **116**, 2490–2500.
- McCreery, D.B., Agnew, W.F., Yuen, T.G.H., and Bullara, L.A. (1988). Comparison of neural damage induced by electrical stimulation with faradaic and capacitor electrodes. *Ann. Biomed. Eng.* **16**, 463–481.
- Feron, K., Lim, R., Sherwood, C., Keynes, A., Brichta, A., and Dastoor, P.C. (2018). Organic bioelectronics: materials and biocompatibility. *Int. J. Mol. Sci.* **19**, 2382.
- Someya, T., Bao, Z., and Malliaras, G.G. (2016). The rise of plastic bioelectronics. *Nature* **540**, 379–385.
- Bettinger, C.J. (2018). Recent advances in materials and flexible electronics for peripheral nerve interfaces. *Bioelectron. Med.* **4**, 6.
- Xie, C., Liu, J., Fu, T.M., Dai, X., Zhou, W., and Lieber, C.M. (2015). Three-dimensional macroporous nanoelectronic networks as minimally invasive brain probes. *Nat. Mater.* **14**, 1286–1292.
- Singh, S., Lo, M.-C., Damodaran, V., Kaplan, H., Kohn, J., Zahn, J., and Shreiber, D. (2016). Modeling the insertion mechanics of flexible neural probes coated with sacrificial polymers for optimizing probe design. *Sensors (Basel)* **16**, 330.
- Pan, L., Wang, F., Cheng, Y., Leow, W.R., Zhang, Y.W., Wang, M., Cai, P., Ji, B., Li, D., and Chen, X. (2020a). A supertough electro-tendon based on spider silk composites. *Nat. Commun.* **11**, 1332.
- Prodanov, D., and Delbecke, J. (2016). Mechanical and biological interactions of implants with the brain and their impact on implant design. *Front. Neurosci.* **10**, 11.
- Nolta, N.F., Ghelich, P., and Han, M. (2019). Recessed traces for planarized passivation of chronic neural microelectrodes. In *Proceedings of the 41st Annual International Conference of the IEEE Engineering in Medicine and Biology Society (EMBC) (IEEE)*, pp. 5125–5128.
- Lee, S.M., Kim, J.H., Park, C., Hwang, J.Y., Hong, J.S., Lee, K.H., and Lee, S.H. (2016). Self-adhesive and capacitive carbon nanotube-based electrode to record electroencephalograph signals from the hairy scalp. *IEEE Trans. Biomed. Eng.* **63**, 138–147.
- Zou, Y., Dehngang, O., Nathan, V., and Jafari, R. (2014). Automatic removal of EEG artifacts using electrode-scalp impedance. In *2014 IEEE International Conference on Acoustics, Speech and Signal Processing (ICASSP) (IEEE)*, pp. 2054–2058.
- Drees, C., Makic, M.B., Case, K., Mancuso, M.P., Hill, A., Walczak, P., Limon, S., Biesecker, K., and Frey, L. (2016). Skin irritation during video-EEG monitoring. *Neurodiagn. J.* **56**, 139–150.
- Lau-Zhu, A., Lau, M.P.H., and McLoughlin, G. (2019). Mobile EEG in research on neurodevelopmental disorders: opportunities and challenges. *Dev. Cogn. Neurosci.* **36**, 100635.
- Bhattarai, S.R., Bhattarai, N., Viswanathamurthi, P., Yi, H.K., Hwang, P.H., and Kim, H.Y. (2006). Hydrophilic nanofibrous structure of polylactide; fabrication and cell affinity. *J. Biomed. Mater. Res. A* **78**, 247–257.
- Fang, Y., Li, X., and Fang, Y. (2015). Organic bioelectronics for neural interfaces. *J. Mater. Chem. C* **3**, 6424–6430.

30. Abidian, M.R., and Martin, D.C. (2008). Experimental and theoretical characterization of implantable neural microelectrodes modified with conducting polymer nanotubes. *Biomaterials* 29, 1273–1283.
31. Liu, J., Fu, T.M., Cheng, Z., Hong, G., Zhou, T., Jin, L., Duvvuri, M., Jiang, Z., Kruskal, P., Xie, C., et al. (2015). Syringe-injectable electronics. *Nat. Nanotechnol.* 10, 629–635.
32. Zhao, S., Tseng, P., Grasman, J., Wang, Y., Li, W., Napier, B., Yavuz, B., Chen, Y., Howell, L., Rincon, J., et al. (2018). Programmable hydrogel ionic circuits for biologically matched electronic interfaces. *Adv. Mater.* 30, 1800598.
33. Oh, J.Y., Kim, S., Baik, H.K., and Jeong, U. (2016). Conducting polymer dough for deformable electronics. *Adv. Mater.* 28, 4455–4461.
34. Ahn, Y., Lee, H., Lee, D., and Lee, Y. (2014). Highly conductive and flexible silver nanowire-based microelectrodes on biocompatible hydrogel. *ACS Appl. Mater. Interfaces* 6, 18401–18407.
35. Park, J., Choi, S., Janardhan, A.H., Lee, S.Y., Raut, S., Soares, J., Shin, K., Yang, S., Lee, C., Kang, K.W., et al. (2016). Electromechanical cardioplasty using a wrapped elastoconductive epicardial mesh. *Sci. Transl. Med.* 8, 344ra86.
36. Chapman, C.A.R., Aristovich, K., Donega, M., Fjordbakk, C.T., Stathopoulou, T.R., Viscasillas, J., et al. (2019). Electrode fabrication and interface optimization for imaging of evoked peripheral nervous system activity with electrical impedance tomography (EIT). *J. Neural Eng.* 16, 016001.
37. Ji, B., Guo, Z., Wang, M., Yang, B., Wang, X., Li, W., et al. (2018). Flexible polyimide-based hybrid opto-electric neural interface with 16 channels of micro-LEDs and electrodes. *Microsyst. Nanoeng.* 4, <https://doi.org/10.1038/s41378-018-0027-0>.
38. Ganji, M., Tanaka, A., Gilja, V., Halgren, E., and Dayeh, S.A. (2017). Scaling effects on the electrochemical stimulation performance of Au, Pt, and PEDOT:PSS electrocorticography arrays. *Adv. Funct. Mater.* 27, 1703019.
39. Ganji, M., Kaestner, E., Hermiz, J., Rogers, N., Tanaka, A., Cleary, D., Lee, S.H., Snider, J., Halgren, M., Cosgrove, G.R., et al. (2018). Development and translation of PEDOT:PSS microelectrodes for intraoperative monitoring. *Adv. Funct. Mater.* 28, 1700232.
40. Lang, U., Naujoks, N., and Dual, J. (2009). Mechanical characterization of PEDOT:PSS thin films. *Synth. Met.* 159, 473–479.
41. Alegret, N., Dominguez-Alfaro, A., González-Dominguez, J.M., Arnaiz, B., Cossio, U., Bosi, S., et al. (2018). Three-Dimensional Conductive Scaffolds as Neural Prostheses Based on Carbon Nanotubes and Polypyrrole. *ACS Appl. Mater. Interfaces.* 10, 43904–43914.
42. Foroughi J., Ghorbani S.R., Peleckis G., Spinks G.M., Wallace G.G., Wang X.L., et al. The mechanical and the electrical properties of conducting polypyrrole fibers. *J. Appl. Phys.* 107, 103712.
43. Kojabad, Z.D., and Shojaosadati, S.A. (2015). Chemical Synthesis of Polypyrrole Nanotubes for Neural Microelectrodes. *Procedia Mater. Sci.* 11, 147–151.
44. Sakurai, T., Toyoshima, S., Kitazume, H., Masuda, S., Kato, H., and Akimoto, K. (2010). Influence of gap states on electrical properties at interface between bathocuproine and various types of metals. *J. Appl. Phys.* 107, 043707.
45. Rivnay, J., Wang, H., Fenno, L., Deisseroth, K., and Malliaras, G.G. (2017). Next-generation probes, particles, and proteins for neural interfacing. *Sci. Adv.* 3, e1601649.
46. Yuk, H., Lu, B., and Zhao, X. (2019). Hydrogel bioelectronics. *Chem. Soc. Rev.* 48, 1642–1667.
47. Lu, Y., Wang, D., Li, T., Zhao, X., Cao, Y., Yang, H., et al. (2009). Poly(vinyl alcohol)/poly(acrylic acid) hydrogel coatings for improving electrode-neural tissue interface. *Biomaterials.* 30, 4143–4151.
48. Kleber, C., Bruns, M., Lienkamp, K., Rühle, J., and Asplund, M. (2017). An interpenetrating, microstructurable and covalently attached conducting polymer hydrogel for neural interfaces. *Acta Biomater.* 58, 365–375.
49. Liu, Y., Liu, J., Chen, S., Lei, T., Kim, Y., Niu, S., Wang, H., Wang, X., Foudeh, A.M., Tok, J.B.H., et al. (2019). Soft and elastic hydrogel-based microelectronics for localized low-voltage neuromodulation. *Nat. Biomed. Eng.* 3, 58–68.
50. Stavrinidou, E., Leleux, P., Rajaona, H., Khodagholy, D., Rivnay, J., Lindau, M., Sanaur, S., and Malliaras, G.G. (2013). Direct measurement of ion mobility in a conducting polymer. *Adv. Mater.* 25, 4488–4493.
51. Cha, C., Shin, S.R., Annabi, N., Dokmeci, M.R., and Khademhosseini, A. (2013). Carbon-based nanomaterials: multifunctional materials for biomedical engineering. *ACS Nano* 7, 2891–2897.
52. Gaharwar, A.K., Peppas, N.A., and Khademhosseini, A. (2014). Nanocomposite hydrogels for biomedical applications. *Biotechnol. Bioeng.* 111, 441–453.
53. Rafieian, S., Mirzadeh, H., Mahdavi, H., and Masoumi, M.E. (2019). A review on nanocomposite hydrogels and their biomedical applications. *IEEE J. Sel. Top. Quan. Electron.* 26, 154–174.
54. Xu, C., Ma, B., Yuan, S., Zhao, C., and Liu, H. (2020). High-Resolution Patterning of Liquid Metal on Hydrogel for Flexible, Stretchable, and Self-Healing Electronics. *Adv. Electron. Mater.* 6, 1900721.
55. Zhou, Y., Wan, C., Yang, Y., Yang, H., Wang, S., Dai, Z., et al. (2019). Highly Stretchable, Elastic, and Ionic Conductive Hydrogel for Artificial Soft Electronics. *Adv. Funct. Mater.* 29, 1806220.
56. Choi, S., Han, S.I., Jung, D., Hwang, H.J., Lim, C., Bae, S., Park, O.K., Tschabrunn, C.M., Lee, M., Bae, S.Y., et al. (2018). Highly conductive, stretchable and biocompatible Ag-Au core-sheath nanowire composite for wearable and implantable bioelectronics. *Nat. Nanotechnol.* 13, 1048–1056.
57. Joo, H., Jung, D., Sunwoo, S.H., Koo, J.H., and Kim, D.H. (2020). Material design and fabrication strategies for stretchable metallic nanocomposites. *Small* 16, 1906270.
58. Parameswaran, R., Koehler, K., Rotenberg, M.Y., Burke, M.J., Kim, J., Jeong, K.Y., Hissa, B., Paul, M.D., Moreno, K., Sarma, N., et al. (2019). Optical stimulation of cardiac cells with a polymer-supported silicon nanowire matrix. *Proc. Natl. Acad. Sci. U S A* 116, 413–421.
59. Sunwoo, S.H., Han, S.I., Kang, H., Cho, Y.S., Jung, D., Lim, C., Lim, C., Cha, M.J., Lee, S.P., Hyeon, T., et al. (2020). Stretchable low-impedance nanocomposite comprised of Ag-Au core-shell nanowires and Pt black for epicardial recording and stimulation. *Adv. Mater. Technol.* 5, 1900768.
60. Kim, D.H., and Rogers, J.A. (2009). Bend, buckle, and fold: mechanical engineering with nanomembranes. *ACS Nano* 3, 498–501.
61. Wang, S., Song, J., Kim, D.H., Huang, Y., and Rogers, J.A. (2008). Local versus global buckling of thin films on elastomeric substrates. *Appl. Phys. Lett.* 93, 023126.
62. Choi, C., Lee, Y., Cho, K.W., Koo, J.H., and Kim, D.H. (2019a). Wearable and implantable soft bioelectronics using two-dimensional materials. *Acc. Chem. Res.* 52, 73–81.
63. Kim, D.H., Lu, N., Ma, R., Kim, Y.S., Kim, R.H., Wang, S., Wu, J., Won, S.M., Tao, H., Islam, A., et al. (2011). Epidermal electronics. *Science* 333, 838–843.
64. Kim, D.H., Viventi, J., Amsden, J.J., Xiao, J., Vigeland, L., Kim, Y.S., Blanco, J.A., Panilaitis, B., Frechette, E.S., Contreras, D., et al. (2010). Dissolvable films of silk fibroin for ultrathin conformal bio-integrated electronics. *Nat. Mater.* 9, 511–517.
65. Petit-Pierre, G., Bertsch, A., and Renaud, P. (2016). Neural probe combining microelectrodes and a droplet-based microdialysis collection system for high temporal resolution sampling. *Lab Chip* 16, 917–924.
66. Lee, H.J., Son, Y., Kim, J., Lee, C.J., Yoon, E.S., and Cho, I.J. (2015). A multichannel neural probe with embedded microfluidic channels for simultaneous in vivo neural recording and drug delivery. *Lab Chip* 15, 1590–1597.
67. Lee, Y., Kim, J., Joo, H., Raj, M.S., Ghaffari, R., and Kim, D.-H. (2017). Wearable sensing systems with mechanically soft assemblies of nanoscale materials. *Adv. Mater. Technol.* 2, 1700053.
68. Ulyanova, A.V., Cottone, C., Adam, C.D., Gagnon, K.G., Cullen, D.K., Holtzman, T., Jamieson, B.G., Koch, P.F., Chen, H.I., Johnson, V.E., et al. (2019). Multichannel silicon probes for awake hippocampal recordings in large animals. *Front. Neurosci.* 13, 397.
69. Lee, H., Bellamkonda, R.V., Sun, W., and Levenston, M.E. (2005). Biomechanical analysis of silicon microelectrode-induced strain in the brain. *J. Neural Eng.* 2, 81–89.
70. Kozai, T.D.Y., Langhals, N.B., Patel, P.R., Deng, X., Zhang, H., Smith, K.L., Lahann, J., Kotov, N.A., and Kipke, D.R. (2012). Ultrasmall implantable composite microelectrodes with

- bioactive surfaces for chronic neural interfaces. *Nat. Mater.* **11**, 1065–1073.
71. Rousche, P.J., Pellinen, D.S., Pivin, D.P., Williams, J.C., Vetter, R.J., and Kipke, D.R. (2001). Flexible polyimide-based intracortical electrode arrays with bioactive capability. *IEEE Trans. Biomed. Eng.* **48**, 361–370.
  72. Jackson, A., and Fetz, E.E. (2007). Compact movable microwire array for long-term chronic unit recording in cerebral cortex of primates. *J. Neurophysiol.* **98**, 3109–3118.
  73. Polikov, V.S., Tresco, P.A., and Reichert, W.M. (2005). Response of brain tissue to chronically implanted neural electrodes. *J. Neurosci. Methods* **148**, 1–18.
  74. Wellman, S.M., Eles, J.R., Ludwig, K.A., Seymour, J.P., Michelson, N.J., McFadden, W.E., Vazquez, A.L., and Kozai, T.D.Y. (2018). A materials roadmap to functional neural interface design. *Adv. Funct. Mater.* **28**, 1701269.
  75. Kim, D.H., Richardson-Burns, S.M., Hendricks, J.L., Sequera, C., and Martin, D.C. (2007). Effect of immobilized nerve growth factor on conductive polymers: electrical properties and cellular response. *Adv. Funct. Mater.* **17**, 79–86.
  76. Pan, S., Zhang, F., Cai, P., Wang, M., He, K., Luo, Y., Li, Z., Chen, G., Ji, S., Liu, Z., et al. (2020b). Mechanically interlocked hydrogel-elastomer hybrids for on-skin electronics. *Adv. Funct. Mater.* **30**, 1909540.
  77. Feiner, R., and Dvir, T. (2017). Tissue-electronics interfaces: from implantable devices to engineered tissues. *Nat. Rev. Mater.* **3**, 17076.
  78. Lacour, S.P., Courtine, G., and Guck, J. (2016). Materials and technologies for soft implantable neuroprostheses. *Nat. Rev. Mater.* **1**, 16063.
  79. Choi, S., Han, S.I., Kim, D., Hyeon, T., and Kim, D.H. (2019b). High-performance stretchable conductive nanocomposites: materials, processes, and device applications. *Chem. Soc. Rev.* **48**, 1566–1595.
  80. Kozai, T.D.Y., Jaquins-Gerstl, A.S., Vazquez, A.L., Michael, A.C., and Cui, X.T. (2015). Brain tissue responses to neural implants impact signal sensitivity and intervention strategies. *ACS Chem. Neurosci.* **6**, 48–67.
  81. Wellman, S.M., and Kozai, T.D.Y. (2017). Understanding the inflammatory tissue reaction to brain implants to improve neurochemical sensing performance. *ACS Chem. Neurosci.* **8**, 2578–2582.
  82. Alba, N.A., Scلابassi, R.J., Sun, M., and Cui, X.T. (2010). Novel hydrogel-based preparation-free EEG electrode. *IEEE Trans. Neural Syst. Rehabil. Eng.* **18**, 415–423.
  83. Benti, S.A., and Dupaix, R.B. (2018). Simulations of hydrogel-coated neural microelectrodes to assess biocompatibility improvement using strain as a metric for micromotion. *Biomed. Phys. Eng. Express* **4**, 035036.
  84. Keplinger, C., Sun, J.Y., Foo, C.C., Rothmund, P., Whitesides, G.M., and Suo, Z. (2013). Stretchable, transparent, ionic conductors. *Science* **341**, 984–987.
  85. Guo, L., Ma, M., Zhang, N., Langer, R., and Anderson, D.G. (2014). Stretchable polymeric multielectrode array for conformal neural interfacing. *Adv. Mater.* **26**, 1427–1433.
  86. Stoyanov, H., Kolloosche, M., Risse, S., Waché, R., and Kofod, G. (2013). Soft conductive elastomer materials for stretchable electronics and voltage controlled artificial muscles. *Adv. Mater.* **25**, 578–583.
  87. Lipomi, D.J., Lee, J.A., Vosgueritchian, M., Tee, B.C.K., Bolander, J.A., and Bao, Z. (2012). Electronic properties of transparent conductive films of PEDOT:PSS on stretchable substrates. *Chem. Mater.* **24**, 373–382.
  88. Tomczykowa, M., and Plonska-Brzezinska, M.E. (2019). Conducting polymers, hydrogels and their composites: preparation, properties and bioapplications. *Polymers (Basel)* **11**, 350.
  89. Rivnay, J., Leleux, P., Ferro, M., Sessolo, M., Williamson, A., Koutsouras, D.A., Khodagholy, D., Ramuz, M., Strakosas, X., Owens, R.M., et al. (2015). High-performance transistors for bioelectronics through tuning of channel thickness. *Sci. Adv.* **1**, e1400251.
  90. Kayser, L.V., and Lipomi, D.J. (2019). Stretchable conductive polymers and composites based on PEDOT and PEDOT:PSS. *Adv. Mater.* **31**, 1806133.
  91. Lee, J.H., Jeong, Y.R., Lee, G., Jin, S.W., Lee, Y.H., Hong, S.Y., Park, H., Kim, J.W., Lee, S.S., and Ha, J.S. (2018a). Highly conductive, stretchable, and transparent PEDOT:PSS electrodes fabricated with triblock copolymer additives and acid treatment. *ACS Appl. Mater. Interfaces* **10**, 28027–28035.
  92. McQuade, J., and Vuong, L.T. (2018). Solvent retention and crack evolution in dropcast PEDOT:PSS and dependence on surface wetting. *ACS Omega* **3**, 3868–3873.
  93. Lu, B., Yuk, H., Lin, S., Jian, N., Qu, K., Xu, J., and Zhao, X. (2019). Pure PEDOT:PSS hydrogels. *Nat. Commun.* **10**, 1043.
  94. Fu, Q., Stein, M., Li, W., Zheng, J., and Kruijs, F.E. (2020). Conductive films prepared from inks based on copper nanoparticles synthesized by transferred arc discharge. *Nanotechnology* **31**, 025302.
  95. Nam, J., Lim, H.K., Kim, N.H., Park, J.K., Kang, E.S., Kim, Y.T., Heo, C., Lee, O.S., Kim, S.G., Yun, W.S., et al. (2020). Supramolecular peptide hydrogel-based soft neural interface augments brain signals through a three-dimensional electrical network. *ACS Nano* **14**, 664–675.
  96. Kim, D.C., Shim, H.J., Lee, W., Koo, J.H., and Kim, D.H. (2020). Material-based approaches for the fabrication of stretchable electronics. *Adv. Mater.* **32**, 1902743.
  97. Kim, S.H., Seo, H., Kang, J., Hong, J., Seong, D., Kim, H.J., Kim, J., Mun, J., Youn, I., Kim, J., et al. (2019). An ultrastretchable and self-healable nanocomposite conductor enabled by autonomously percolative electrical pathways. *ACS Nano* **13**, 6531–6539.
  98. Niu, S., Matsuhiha, N., Beker, L., Li, J., Wang, S., Wang, J., Jiang, Y., Yan, X., Yun, Y., Burnett, W., et al. (2019). A wireless body area sensor network based on stretchable passive tags. *Nat. Electron.* **2**, 361–368.
  99. Cha, G.D., Kang, D., Lee, J., and Kim, D.H. (2019). Bioresorbable electronic implants: history, materials, fabrication, devices, and clinical applications. *Adv. Healthc. Mater.* **8**, 1801660.
  100. Berkowski, K.L., Plunkett, K.N., Yu, Q., and Moore, J.S. (2005). Introduction to photolithography: preparation of microscale polymer silhouettes. *J. Chem. Educ.* **82**, 1365–1369.
  101. Hwang, S.W., Kim, D.H., Tao, H., Kim, T.I., Kim, S., Yu, K.J., Panilaitis, B., Jeong, J.W., Song, J.K., Omenetto, F.G., et al. (2013). Materials and fabrication processes for transient and bioresorbable high-performance electronics. *Adv. Funct. Mater.* **23**, 4087–4093.
  102. Viventi, J., Kim, D.H., Vigeland, L., Frechette, E.S., Blanco, J.A., Kim, Y.S., Avrin, A.E., Tiruvadi, V.R., Hwang, S.W., Vanleer, A.C., et al. (2011). Flexible, foldable, actively multiplexed, high-density electrode array for mapping brain activity in vivo. *Nat. Neurosci.* **14**, 1599–1605.
  103. Hahn, M.S., Taite, L.J., Moon, J.J., Rowland, M.C., Ruffino, K.A., and West, J.L. (2006). Photolithographic patterning of polyethylene glycol hydrogels. *Biomaterials* **27**, 2519–2524.
  104. Lim, C., Shin, Y., Jung, J., Kim, J.H., Lee, S., and Kim, D.H. (2019). Stretchable conductive nanocomposite based on alginate hydrogel and silver nanowires for wearable electronics. *APL Mater.* **7**, 031502.
  105. Rahimi, R., Shams Es-haghi, S., Chittiboyina, S., Mutlu, Z., Lelièvre, S.A., Cakmak, M., and Ziaie, B. (2018). Laser-enabled processing of stretchable electronics on a hydrolytically degradable hydrogel. *Adv. Healthc. Mater.* **7**, 1800231.
  106. Yang, Y., Song, Y., Bo, X., Min, J., Pak, O.S., Zhu, L., Wang, M., Tu, J., Kogan, A., Zhang, H., et al. (2020). A laser-engraved wearable sensor for sensitive detection of uric acid and tyrosine in sweat. *Nat. Biotechnol.* **38**, 217–224.
  107. Pan, C., Kumar, K., Li, J., Markvicka, E.J., Herman, P.R., and Majidi, C. (2018). Visually imperceptible liquid-metal circuits for transparent, stretchable electronics with direct laser writing. *Adv. Mater.* **30**, 1706937.
  108. Henle, C., Raab, M., Cordeiro, J.G., Doostkam, S., Schulze-Bonhage, A., Stieglitz, T., and Rickert, J. (2011). First long term in vivo study on subdurally implanted Micro-ECOG electrodes, manufactured with a novel laser technology. *Biomed. Microdevices* **13**, 59–68.
  109. Munarin, F., Kaiser, N.J., Kim, T.Y., Choi, B.R., and Coulombe, K.L.K. (2017). Laser-etched designs for molding hydrogel-based engineered tissues. *Tissue Eng. Part C Methods* **23**, 311–321.
  110. Ashby, M., Ferreira, P., and Schodek, D.L. (2009). *Nanomaterials, Nanotechnologies and Design: An Introduction for Engineers and*

- Architects (Elsevier). <https://doi.org/10.1016/B978-0-7506-8149-0.X0001-3>.
111. Gribi, S., du Bois de Dunilac, S., Ghezzi, D., and Lacour, S.P. (2018). A microfabricated nerve-on-a-chip platform for rapid assessment of neural conduction in explanted peripheral nerve fibers. *Nat. Commun.* **9**, 4403.
  112. Sahin, O., Ashokkumar, M., and Ajayan, P.M. (2018). Micro- and nanopatterning of biomaterial surfaces. In *Fundamental Biomaterials: Metals*, P. Balakrishnan, M.S. Sreekala, and S. Thomas, eds. (Woodhead Publishing), pp. 67–78.
  113. Lee, J.S., Kang, S.J., Shin, J.H., Shin, Y.J., Lee, B., Koo, J.M., and Kim, T. (2020b). Nanoscale-dewetting-based direct interconnection of microelectronics for a deterministic assembly of transfer printing. *Adv. Mater.* **32**, 1908422.
  114. Qiao, S., and Lu, N. (2016). Stress analysis for nanomembranes under stamp compression. *Extrem. Mech. Lett.* **7**, 136–144.
  115. McCall, J.G., Kim, T.I., Shin, G., Huang, X., Jung, Y.H., Al-Hasani, R., Omenetto, F.G., Bruchas, M.R., and Rogers, J.A. (2013). Fabrication and application of flexible, multimodal light-emitting devices for wireless optogenetics. *Nat. Protoc.* **8**, 2413–2428.
  116. Song, J.K., Do, K., Koo, J.H., Son, D., and Kim, D.H. (2019a). Nanomaterials-based flexible and stretchable bioelectronics. *MRS Bull.* **44**, 643–664.
  117. Joo, H., Shin, J., Cho, S.W., and Kim, P. (2016). Wrinkled-surface mediated reverse transfection platform for highly efficient, addressable gene delivery. *Adv. Healthc. Mater.* **5**, 2025–2030.
  118. Kim, S.J., Cho, H.R., Cho, K.W., Qiao, S., Rhim, J.S., Soh, M., Kim, T., Choi, M.K., Choi, C., Park, I., et al. (2015). Multifunctional cell-culture platform for aligned cell sheet monitoring, transfer printing, and therapy. *ACS Nano* **9**, 2677–2688.
  119. Choi, S., Lee, H., Ghaffari, R., Hyeon, T., and Kim, D.H. (2016). Recent advances in flexible and stretchable bio-electronic devices integrated with nanomaterials. *Adv. Mater.* **28**, 4203–4218.
  120. Choi, S., Park, J., Hyun, W., Kim, J., Kim, J., Lee, Y.B., Song, C., Hwang, H.J., Kim, J.H., Hyeon, T., et al. (2015). Stretchable heater using ligand-exchanged silver nanowire nanocomposite for wearable articular thermotherapy. *ACS Nano* **9**, 6626–6633.
  121. Mineev, I.R., Musienko, P., Hirsch, A., Barraud, Q., Wenger, N., Moraud, E.M., Gandar, J., Capogrosso, M., Milekovic, T., Asboth, L., et al. (2015). Electronic dura mater for long-term multimodal neural interfaces. *Science* **347**, 159–163.
  122. Adly, N., Weidlich, S., Seyock, S., Brings, F., Yakushenko, A., Offenhüsser, A., and Wolf, B. (2018). Printed microelectrode arrays on soft materials: from PDMS to hydrogels. *Npj Flex. Electron.* **2**, 15.
  123. Truby, R.L., and Lewis, J.A. (2016). Printing soft matter in three dimensions. *Nature* **540**, 371–378.
  124. Lee, J.H., Kim, H., Hwang, J.Y., Chung, J., Jang, T.M., Seo, D.G., Gao, Y., Lee, J., Park, H., Lee, S., et al. (2020a). 3D printed, customizable, and multifunctional smart electronic eyeglasses for wearable healthcare systems and human-machine interfaces. *ACS Appl. Mater. Interfaces* **12**, 21424–21432.
  125. Li, J., Wu, C., Chu, P.K., and Gelinsky, M. (2020). 3D printing of hydrogels: rational design strategies and emerging biomedical applications. *Mater. Sci. Eng. R Rep.* **140**, 100543.
  126. Wu, T., Gray, E., and Chen, B. (2018). A self-healing, adaptive and conductive polymer composite ink for 3D printing of gas sensors. *J. Mater. Chem. C* **6**, 6200–6207.
  127. Yuk, H., Lu, B., Lin, S., Qu, K., Xu, J., Luo, J., and Zhao, X. (2020). 3D printing of conducting polymers. *Nat. Commun.* **11**, 1604.
  128. Jung, Y.H., Kim, J.U., Lee, J.S., Shin, J.H., Jung, W., Ok, J., and Kim, T.I. (2020). Injectable biomedical devices for sensing and stimulating internal body organs. *Adv. Mater.* **32**, 1907478.
  129. Sanei, S., and Chambers, J.A. (2013). *EEG Signal Processing* (John Wiley & Sons Ltd).
  130. Ha, S., Kim, C., Mercier, P.P., and Cauwenberghs, G. (2019). High-Density Integrated Electro cortical Neural Interfaces: Low-Noise Low-Power System-On-Chip Design Methodology (Elsevier).
  131. Telenczuk, B., Dehghani, N., Le Van Quyen, M., Cash, S.S., Halgren, E., Hatsopoulos, N.G., and Destexhe, A. (2017). Local field potentials primarily reflect inhibitory neuron activity in human and monkey cortex. *Sci. Rep.* **7**, 40211.
  132. Buzsáki, G., Anastassiou, C.A., and Koch, C. (2012). The origin of extracellular fields and currents—EEG, ECoG, LFP and spikes. *Nat. Rev. Neurosci.* **13**, 407–420.
  133. Norton, J.J.S., Lee, D.S., Lee, J.W., Lee, W., Kwon, O., Won, P., Jung, S.Y., Cheng, H., Jeong, J.W., Akce, A., et al. (2015). Soft, curved electrode systems capable of integration on the auricle as a persistent brain-computer interface. *Proc. Natl. Acad. Sci. U S A* **112**, 3920–3925.
  134. Lee, M., Shim, H.J., Choi, C., and Kim, D.H. (2019b). Soft high-resolution neural interfacing probes: materials and design approaches. *Nano Lett.* **19**, 2741–2749.
  135. Biasucci, A., Franceschiello, B., and Murray, M.M. (2019). Electroencephalography. *Curr. Biol.* **29**, R80–R85.
  136. O’Sullivan, M., Temko, A., Bocchino, A., O’Mahony, C., Boylan, G., and Popovici, E. (2019). Analysis of a low-cost EEG monitoring system and dry electrodes toward clinical use in the neonatal ICU. *Sensors (Basel)* **19**, 2637.
  137. Gao, K.-P., Yang, H.-J., Wang, X.-L., Yang, B., and Liu, J.-Q. (2018). Soft pin-shaped dry electrode with bristles for EEG signal measurements. *Sens. Actuators A Phys.* **283**, 348–361.
  138. Chen, Y.H., Op de Beeck, M., Vanderheyden, L., Carrette, E., Mihajlović, V., Vanstreels, K., Grundlehner, B., Gadeyne, S., Boon, P., and van Hoof, C. (2014). Soft, comfortable polymer dry electrodes for high quality ECG and EEG recording. *Sensors (Basel)* **14**, 23758–23780.
  139. Ma, R., Kim, D.H., McCormick, M., Coleman, T., and Rogers, J. (2010). A stretchable electrode array for non-invasive, skin-mounted measurement of electrocardiography (ECG), electromyography (EMG) and electroencephalography (EEG). In *2010 Annual International Conference of the IEEE Engineering in Medicine and Biology Society, EMBC’10 (IEEE)*, pp. 6405–6408.
  140. Tian, L., Zimmerman, B., Akhtar, A., Yu, K.J., Moore, M., Wu, J., Larsen, R.J., Lee, J.W., Li, J., Liu, Y., et al. (2019). Large-area MRI-compatible epidermal electronic interfaces for prosthetic control and cognitive monitoring. *Nat. Biomed. Eng.* **3**, 194–205.
  141. Gunduz, A., Brunner, P., Daitch, A., Leuthardt, E.C., Ritaccio, A.L., Pesaran, B., and Schalk, G. (2012). Decoding covert spatial attention using electrocorticographic (ECoG) signals in humans. *Neuroimage* **60**, 2285–2293.
  142. Escabí, M.A., Read, H.L., Viventi, J., Kim, D.-H., Higgins, N.C., Storaice, D.A., Liu, A.S.K., Gifford, A.M., Burke, J.F., Campisi, M., et al. (2014). A high-density, high-channel count, multiplexed  $\mu$ ECoG array for auditory-cortex recordings. *J. Neurophysiol.* **112**, 1566–1583.
  143. Cea, C., Spyropoulos, G.D., Jastrzebska-Perfect, P., Ferrero, J.J., Gelinas, J.N., and Khodagholy, D. (2020). Enhancement-mode ion-based transistor as a comprehensive interface and real-time processing unit for in vivo electrophysiology. *Nat. Mater.* **19**, 679–686.
  144. Spyropoulos, G.D., Gelinas, J.N., and Khodagholy, D. (2020). Internal ion-gated organic electrochemical transistor: a building block for integrated bioelectronics. *Sci. Adv.* **5**, eaau7378.
  145. Hess-Dunning, A., and Tyler, D.J. (2018). A mechanically-adaptive polymer nanocomposite-based intracortical probe and package for chronic neural recording. *Micromachines* **9**, 583.
  146. Vitale, F., Summerson, S.R., Aazhang, B., Kemere, C., and Pasquali, M. (2015). Neural stimulation and recording with bidirectional, soft carbon nanotube fiber microelectrodes. *ACS Nano* **9**, 4465–4474.
  147. Cash, S.S., and Hochberg, L.R. (2015). The emergence of single neurons in clinical neurology. *Neuron* **86**, 79–91.
  148. Sunwoo, S.H., Lee, J.S., Bae, S., Shin, Y.J., Kim, C.S., Joo, S.Y., Choi, H.S., Suh, M., Kim, S.W., Choi, Y.J., et al. (2019). Chronic and acute stress monitoring by electrophysiological signals from adrenal gland. *Proc. Natl. Acad. Sci. U S A* **116**, 1146–1151.
  149. Song, Y., Min, J., and Gao, W. (2019b). Wearable and implantable electronics: moving toward precision therapy. *ACS Nano* **13**, 12280–12286.
  150. Michoud, F., Sottas, L., Browne, L.E., Asboth, L., Latremoliere, A., Sakuma, M., Courtine, G., Wolf, C.J., and Lacour, S.P. (2018). Optical cuff for optogenetic control of the peripheral nervous system. *J. Neural Eng.* **15**, 015002.



151. Vachicouras, N., Tarabichi, O., Kanumuri, V.V., Tringides, C.M., Macron, J., Fallegger, F., Thenaisie, Y., Epprecht, L., McInturff, S., Qureshi, A.A., et al. (2019). Microstructured thin-film electrode technology enables proof of concept of scalable, soft auditory brainstem implants. *Sci. Transl. Med.* **11**, eaax9487.
152. Jonsson, A., Song, Z., Nilsson, D., Meyerson, B.A., Simon, D.T., Linderoth, B., and Berggren, M. (2015). Therapy using implanted organic bioelectronics. *Sci. Adv.* **1**, e1500039.
153. Zhang, Y., Castro, D.C., Han, Y., Wu, Y., Guo, H., Weng, Z., Xue, Y., Austra, J., Wang, X., Li, R., et al. (2019). Battery-free, lightweight, injectable microsystem for in vivo wireless pharmacology and optogenetics. *Proc. Natl. Acad. Sci. U S A* **116**, 21427–21437.
154. Lee, J., Cho, H.R., Cha, G.D., Seo, H., Lee, S., Park, C.K., Kim, J.W., Qiao, S., Wang, L., Kang, D., et al. (2019a). Flexible, sticky, and biodegradable wireless device for drug delivery to brain tumors. *Nat. Commun.* **10**, 5205.
155. Wenger, N., Moraud, E.M., Gandar, J., Musienko, P., Capogrosso, M., Baud, L., Le Goff, C.G., Barraud, Q., Pavlova, N., Dominici, N., et al. (2016). Spatiotemporal neuromodulation therapies engaging muscle synergies improve motor control after spinal cord injury. *Nat. Med.* **22**, 138–145.
156. Russell, C., Roche, A.D., and Chakrabarty, S. (2019). Peripheral nerve bionic interface: a review of electrodes. *Int. J. Intell. Robot. Appl.* **3**, 11–18.
157. Koo, J.H., Jeong, S., Shim, H.J., Son, D., Kim, J., Kim, D.C., Choi, S., Hong, J.I., and Kim, D.H. (2017). Wearable electrocardiogram monitor using carbon nanotube electronics and color-tunable organic light-emitting diodes. *ACS Nano* **11**, 10032–10041.
158. Soffer, E.E. (2012). Gastric electrical stimulation for gastroparesis. *J. Neurogastroenterol. Motil.* **18**, 131–137.
159. Kim, S.J., Cho, K.W., Cho, H.R., Wang, L., Park, S.Y., Lee, S.E., Hyeon, T., Lu, N., Choi, S.H., and Kim, D.H. (2016). Stretchable and transparent biointerface using cell-sheet-graphene hybrid for electrophysiology and therapy of skeletal muscle. *Adv. Funct. Mater.* **26**, 3207–3217.
160. Samidurai, M., Kang, H., Ramasamy, V.S., and Jo, J. (2018). Impact of electrical stimulation on cortisol secretion in rat adrenal gland. *Biochip J.* **12**, 216–221.
161. Abu-Thabit, N.Y., and Makhlof, A.S.H. (2018). Historical development of drug delivery systems: from conventional macroscale to controlled, targeted, and responsive nanoscale systems. In *Stimuli Responsive Polymeric Nanocarriers for Drug Delivery Applications Volume 1: Types and Triggers*, N.Y. Abu-Thabit and A.S.H. Makhlof, eds. (Woodhead Publishing), pp. 3–41.
162. Yun, Y.H., Lee, B.K., and Park, K. (2015). Controlled drug delivery: historical perspective for the next generation. *J. Control. Release* **219**, 2–7.
163. Gao, W., and Wang, J. (2014). Synthetic micro/nanomotors in drug delivery. *Nanoscale* **6**, 10486–10494.
164. Lee, S., Hwang, G., Kim, T.H., Kwon, S.J., Kim, J.U., Koh, K., Park, B., Hong, H., Yu, K.J., Chae, H., et al. (2018b). On-demand drug release from gold nanoturf for a thermo- and chemotherapeutic esophageal stent. *ACS Nano* **12**, 6756–6766.
165. Jena, L., McErlean, E., and McCarthy, H. (2020). Delivery across the blood-brain barrier: nanomedicine for glioblastoma multiforme. *Drug Deliv. Transl. Res.* **10**, 304–318.
166. Upadhyay, R.K. (2014). Drug delivery systems, CNS protection, and the blood brain barrier. *Biomed. Res. Int.* **2014**, <https://doi.org/10.1155/2014/869269>.
167. Qazi, R., Gomez, A.M., Castro, D.C., Zou, Z., Sim, J.Y., Xiong, Y., Abdo, J., Kim, C.Y., Anderson, A., Lohner, F., et al. (2019). Wireless optofluidic brain probes for chronic neuropharmacology and photostimulation. *Nat. Biomed. Eng.* **3**, 655–669.
168. Rustenhoven, J., and Kipnis, J. (2019). Bypassing the blood-brain barrier. *Science* **366**, 1448–1449.
169. Gage, G.J., Stoetznner, C.R., Richner, T., Brodnick, S.K., Williams, J.C., and Kipke, D.R. (2012). Surgical implantation of chronic neural electrodes for recording single unit activity and electrocorticographic signals. *J. Vis. Exp.* **3565**.
170. Musk, E. (2019). An integrated brain-machine interface platform with thousands of channels. *J. Med. Internet Res.* **21**, e16194.
171. Samineni, V.K., Yoon, J., Crawford, K.E., Jeong, Y.R., McKenzie, K.C., Shin, G., Xie, Z., Sundaram, S.S., Li, Y., Yang, M.Y., et al. (2017). Fully implantable, battery-free wireless optoelectronic devices for spinal optogenetics. *Pain* **158**, 2108–2116.